

# Mass Balance of the Greenland and Antarctic Ice Sheets from 1992 to 2020

Inès N. Otosaka<sup>1</sup>, Andrew Shepherd<sup>1</sup>, Erik R. Ivins<sup>2</sup>, Nicole-Jeanne Schlegel<sup>2</sup>, Charles Amory<sup>3</sup>, Michiel R. van den Broeke<sup>4</sup>, Martin Horwath<sup>5</sup>, Ian Joughin<sup>6</sup>, Michalea D. King<sup>6</sup>, Gerhard Krinner<sup>3</sup>, Sophie Nowicki<sup>7</sup>, Antony J. Payne<sup>8</sup>, Eric Rignot<sup>9</sup>, Ted Scambos<sup>10</sup>, Karen M. Simon<sup>11</sup>, Benjamin E. Smith<sup>6</sup>, Louise S. Sørensen<sup>12</sup>, Isabella Velicogna<sup>2,9</sup>, Pippa L. Whitehouse<sup>13</sup>, Geruo A.<sup>9</sup>, Cécile Agosta<sup>14</sup>, Andreas P. Ahlstrøm<sup>15</sup>, Alejandro Blazquez<sup>16</sup>, William Colgan<sup>15</sup>, Marcus E. Engdhal<sup>17</sup>, Xavier Fettweis<sup>18</sup>, Rene Forsberg<sup>12</sup>, Hubert Gallée<sup>3</sup>, Alex Gardner<sup>2</sup>, Lin Gilbert<sup>19</sup>, Noel Gourmelen<sup>20</sup>, Andreas Groh<sup>5</sup>, Brian C. Gunter<sup>21</sup>, Christopher Harig<sup>22</sup>, Veit Helm<sup>23</sup>, Shfaqat Abbas Khan<sup>12</sup>, Christoph Kittel<sup>3</sup>, Hannes Konrad<sup>24</sup>, Peter L. Langen<sup>25</sup>, Benoit S. Lecavalier<sup>26</sup>, Chia-Chun Liang<sup>9</sup>, Bryant D. Loomis<sup>27</sup>, Malcolm McMillan<sup>28</sup>, Daniele Melini<sup>29</sup>, Sebastian H. Mernild<sup>30</sup>, Ruth Mottram<sup>31</sup>, Jeremie Mouginit<sup>3</sup>, Johan Nilsson<sup>2</sup>, Brice Noël<sup>4</sup>, Mark E. Pattle<sup>32</sup>, William R. Peltier<sup>33</sup>, Nadege Pie<sup>34</sup>, Mònica Roca<sup>35</sup>, Ingo Sasgen<sup>23</sup>, Himanshu V. Save<sup>34</sup>, Ki-Weon Seo<sup>36</sup>, Bernd Scheuchl<sup>9</sup>, Ernst J.O. Schrama<sup>37</sup>, Ludwig Schröder<sup>5</sup>, Sebastian B. Simonsen<sup>12</sup>, Thomas Slater<sup>1</sup>, Giorgio Spada<sup>38</sup>, Tyler C. Sutterley<sup>39</sup>, Bramha Dutt Vishwakarma<sup>40</sup>, Melchior van Wessem<sup>4</sup>, David Wiese<sup>2</sup>, Wouter van der Wal<sup>11</sup>, Bert Wouters<sup>11,4</sup>

<sup>1</sup>Centre for Polar Observation and Modelling, University of Leeds, Leeds, United Kingdom

<sup>2</sup>Jet Propulsion Laboratory, California Institute of Technology, Pasadena, United States

<sup>3</sup>Institute of Environmental Geosciences, Université Grenoble Alpes, Grenoble, France

<sup>4</sup>Institute for Marine and Atmospheric Research, Utrecht University, Utrecht, The Netherlands

<sup>5</sup>Institut für Planetare Geodäsie, Technische Universität Dresden, Dresden, Germany

<sup>6</sup>Polar Science Center, University of Washington, Seattle, United States

<sup>7</sup>Department of Geology, University at Buffalo, Buffalo, United States

<sup>8</sup>School of Geographical Sciences, University of Bristol, Bristol, United Kingdom

<sup>9</sup>Earth System Science, University of California Irvine, Irvine, United States

<sup>10</sup>Earth Science and Observation Center, CIRES, University of Colorado Boulder, Boulder, United States

<sup>11</sup>Faculty of Civil Engineering and Geoscience, Delft University of Technology, Delft, The Netherlands

<sup>12</sup>National Space Institute, Technical University of Denmark, Lyngby, Denmark

<sup>13</sup>Department of Geography, Durham University, Durham, United Kingdom

<sup>14</sup>Laboratoire des Sciences du Climat et de l'Environnement, LSCE-IPSL, CEA-CNRS-UVSQ, Gif-sur-Yvette, France

<sup>15</sup>Glaciology and Climate, Geological Survey of Denmark and Greenland, Copenhagen, Denmark

<sup>16</sup>Spatial Geophysics and Oceanography Studies Laboratory, Toulouse, France

<sup>17</sup>ESA-ESRIN, Frascati, Italy

<sup>18</sup>Geography, University of Liège, Liège, Belgium

<sup>19</sup>Mullard Space Science Laboratory, University College London, West Sussex, United Kingdom

<sup>20</sup>University of Edinburgh, Edinburgh, United Kingdom

<sup>21</sup>Aerospace Engineering, Georgia Institute of Technology, Atlanta, United States

<sup>22</sup>Department of Geosciences, University of Arizona, Tucson, United States

<sup>23</sup>Glaciology, Alfred-Wegener-Institute Helmholtz-Center for Polar and Marine Research, Bremerhaven, Germany

<sup>24</sup>Satellite-based Climate Monitoring, Deutscher Wetterdienst, Offenbach/Main, Germany

<sup>25</sup>Department of Environmental Science, iClimate, Aarhus University, Roskilde, Denmark

<sup>26</sup>Department of Physics and Physical Oceanography, Memorial University, St. John's, Canada

<sup>27</sup>Geodesy and Geophysics Laboratory, NASA GSFC, Greenbelt, United States

<sup>28</sup>Lancaster Environment Centre, Lancaster University, Lancaster, United Kingdom

- <sup>29</sup>Istituto Nazionale di Geofisica e Vulcanologia, Rome, Italy
- <sup>30</sup>SDU Climate Cluster, University of Southern Denmark, Odense, Denmark
- <sup>31</sup>Research and Development Department, Danish Meteorological Institute, Copenhagen, Denmark
- <sup>32</sup>isardSAT, Guildford, United Kingdom
- <sup>33</sup>Physics, University of Toronto, Toronto, Canada
- <sup>34</sup>Center for Space Research, University of Texas at Austin, Austin, United States
- <sup>35</sup>isardSAT, Barcelona, Spain
- <sup>36</sup>Department of Earth Science Education, Seoul National University, Seoul, Korea
- <sup>37</sup>Department SpE, Faculty of Aerospace Engineering, TU Delft, Delft, The Netherlands
- <sup>38</sup>Dipartimento di Fisica e Astronomia, Alma Mater Studiorum Università di Bologna, Bologna, Italy
- <sup>39</sup>Applied Physics Laboratory, University of Washington, Seattle, United States
- <sup>40</sup>Interdisciplinary Centre for Water Research, Indian Institute of Science, Bengaluru, India

*Correspondence to:* Inès N. Otosaka (i.n.otosaka@leeds.ac.uk)

5 **Abstract.** Ice losses from the Greenland and Antarctic Ice Sheets have accelerated since the 1990s, accounting  
for a significant increase in global mean sea level. Here, we present a new 29-year record of ice sheet mass balance  
from 1992 to 2020 from the Ice Sheet Mass Balance Inter-comparison Exercise (IMBIE). We compare and  
combine 50 independent estimates of ice sheet mass balance derived from satellite observations of temporal  
changes in ice sheet flow, in ice sheet volume and in Earth's gravity field. Between 1992 and 2020, the ice sheets  
10 contributed  $21.0 \pm 1.9$  mm to global mean sea-level, with the rate of mass loss rising from  $105 \text{ Gt yr}^{-1}$  between  
1992 and 1996 to  $372 \text{ Gt yr}^{-1}$  between 2016 and 2020. In Greenland, the rate of mass loss is  $169 \pm 9 \text{ Gt yr}^{-1}$   
between 1992 and 2020 but there are large inter-annual variations in mass balance with mass loss ranging from  
 $86 \text{ Gt yr}^{-1}$  in 2017 to  $444 \text{ Gt yr}^{-1}$  in 2019 due to large variability in surface mass balance. In Antarctica, ice losses  
continue to be dominated by mass loss from West Antarctica ( $82 \pm 9 \text{ Gt yr}^{-1}$ ) and to a lesser extent from the  
15 Antarctic Peninsula ( $13 \pm 5 \text{ Gt yr}^{-1}$ ). East Antarctica remains close to a state of balance with a small gain of  $3 \pm$   
 $15 \text{ Gt yr}^{-1}$ , but is the most uncertain component of Antarctica's mass balance. The dataset is publicly available at  
<https://doi.org/10.5285/77B64C55-7166-4A06-9DEF-2E400398E452> (The IMBIE Team, 2021).

## 1 Introduction

20 The Antarctic and Greenland Ice Sheets store the vast majority (99%) of Earth's freshwater ice on land. The rate  
of change in ice sheet mass - or ice sheet mass balance - is the net difference between mass loss through solid ice  
discharge at the grounding line, melting at the bed and at the ice-ocean interface and the surface mass balance  
(SMB; precipitation minus meltwater runoff, sublimation, evaporation, and erosion). Over the past three decades  
(between the 1990s and 2010s), ice losses from Antarctica and Greenland increased six-fold (The IMBIE Team,  
25 2018, 2020), raising the global sea level (WCRP Global Sea Level Budget Group, 2018) and with it the risk of  
coastal flooding worldwide (Kulp and Strauss, 2019; Vitousek et al., 2017; Hanson et al., 2011). In Antarctica,  
the losses have arisen primarily due to ocean-driven melting of ice shelves (Adusumilli et al., 2020; Paolo et al.,  
2015) and their collapse (Cook and Vaughan, 2010), which have accelerated the ice flow (Hogg et al., 2017;  
Selley et al., 2021; Rignot et al., 2004), retreat (Konrad et al., 2018; Milillo et al., 2022; Jenkins et al., 2018) and  
30 drawdown (Konrad et al., 2017; Shepherd et al., 2019) of numerous marine-terminating ice streams. In Greenland,  
increasing air temperatures (Hanna et al., 2021) and decreasing cloud cover (Hofer et al., 2017) have exacerbated  
summertime surface melting (Leeson et al., 2015; Tedesco and Fettweis, 2020) and runoff (Trusel et al., 2018;  
Slater et al., 2021), in tandem with the speedup (Rignot and Kanagaratnam, 2006) and retreat (King et al., 2020)  
of outlet glaciers responding to a warming ocean (Straneo and Heimbach, 2013). While ice sheet response to  
35 climate forcing remains the least constrained component of the twenty-first-century sea level budget (Pattyn and  
Morlighem, 2020; Fox-Kemper et al., 2021), maintaining the long-term observational record of ice sheet mass  
balance is critical to improving ice sheet model skill (Edwards et al., 2021; Ritz et al., 2015) and confidence in  
projections of sea level rise (Aschwanden et al., 2021; Slater et al., 2020; Shepherd and Nowicki, 2017).

Thanks to the launch of new satellite missions and the development of improved geophysical corrections and  
40 models of SMB and glacial isostatic adjustment (GIA), it is now possible to routinely monitor ice sheet mass  
changes using observations of ice-flow derived from satellite radar and optical imagery (e.g. Gardner et al., 2018;  
Moon et al., 2012; Mouginot et al., 2017), surface elevation changes (derived from satellite altimetry) (e.g.

Sandberg Sørensen et al., 2018; Smith et al., 2020), and fluctuations in Earth's gravity field (derived from satellite gravimetry from GRACE and its follow on) (e.g. Tapley et al., 2019; Velicogna et al., 2020; Sasgen et al., 2020).  
45 The Ice Sheet Mass Balance Inter-comparison Exercise (IMBIE) has shown that there is good agreement between these satellite methods (Shepherd et al., 2012) and that combining independent satellite-based ice sheet mass balance estimates reduces uncertainty in estimates of Greenland and Antarctica's contribution to sea level rise. By adopting a common framework to support the comparison and aggregation of ice sheet mass balance estimates generated by different participants, it is possible to assess differences between techniques and the impact of using  
50 different geophysical corrections, SMB models, or GIA models in ice sheet mass balance estimation to produce a reconciled time-series of ice sheet mass changes. SMB models are required for estimating the net mass balance in the input-output method while GIA models are necessary to correct ice sheet mass balance estimates derived from satellite gravimetry and to a lesser extent those derived from satellite altimetry. The GIA is the result of solid Earth mass redistribution caused by changes in ice mass since the last glaciation. Gravimetry fields record the combined effect of mass redistribution due to the GIA and recent changes in ice sheet mass balance. The GIA  
55 contribution therefore needs to be modelled separately and removed from the gravimetry fields, especially since it is of the same order of magnitude as the ice sheet mass balance signal (Caron and Ivins, 2020; Sutterley et al., 2014a). Altimetry elevation change estimates also need to be corrected for the GIA. However, contrary to gravimetry estimates, altimetry estimates are less sensitive to GIA as it manifests as an uplift (or subsidence) rate  
60 of the order of a few millimetres per year, much smaller than the elevation changes recorded. The most recent IMBIE assessments for the Antarctic Ice Sheet and the Greenland Ice Sheet covered the periods 1992 to 2017 and 1992 to 2018, respectively, and reported a combined contribution of  $17.8 \pm 1.8$  mm to global mean sea level (GMSL) between 1992 and 2017 (The IMBIE Team, 2018, 2020). Here, we extend these records to cover the same extended period (1<sup>st</sup> January 1992 to 31<sup>st</sup> December 2020) for both ice sheets. In the rest of the paper, all of  
65 time periods cited refer to the period extending from 1<sup>st</sup> January of the first year quoted to 31<sup>st</sup> December of the second year quoted.

In the years since our most recent assessment there have been notable changes in ice sheet mass in both hemispheres, and in the availability of satellite observations and ancillary datasets with which to detect these changes. In Greenland, for example, atmospheric blocking and reduced summertime snowfall (Tedesco and  
70 Fettweis, 2020) led to near-record levels of meltwater runoff in 2019 (Slater et al., 2021) which, in combination with progressively increasing ice discharge (Mouginot et al., 2019), set a new record for annual ice losses during the satellite era (Sasgen et al., 2020). In Antarctica, pervasive mass losses have continued in the Amundsen Sea Sector (Groh and Horwath, 2021) as a consequence of further grounding line retreat (Milillo et al., 2022) and the associated glacier speedup (Joughin et al., 2021). A follow on to the GRACE satellite mission (GRACE-FO) was  
75 launched in May 2018 (Tapley et al., 2019), the ICESat-2 satellite laser altimeter mission was launched in September 2018 (Smith et al., 2020), and updated products have been released for many others - including swath altimetry from CryoSat-2 (Gourmelen et al., 2018). To accompany these observations, there have been updated models of GIA (e.g. Caron and Ivins, 2020) to correct mass and elevation changes associated with solid earth movement, of firn densification (e.g. Stevens et al., 2020) to correct changes in elevation for surface processes,  
80 and of SMB (e.g. Fettweis et al., 2020; Mottram et al., 2021) to aid mass budget and mass balance partitioning calculations.

Here, we make use of new satellite observations, new methods and models to provide an updated IMBIE assessment of Greenland and Antarctic ice sheet mass balance, extending our most recent records by 3 and 4 years, respectively. We provide a description of the datasets incorporated in this updated assessment and of the aggregation methods employed. We also discuss differences between the ice sheet mass balance estimates derived from altimetry, gravimetry and the input-output method, and we present extended reconciled time-series of ice sheet mass change. We discuss the limitations of our dataset and outline a roadmap for future improvements. Finally, we contrast our findings with trends in GMSL and compare them with projections of future ice sheet mass changes from the Intergovernmental Panel on Climate Change's (IPCC) Sixth Assessment Report (AR6).

## 2 Data

### 2.1 Data Background

Fluctuations in ice sheet mass are a key indicator of ice sheet stability and can be inferred using a range of satellite techniques (Shepherd et al., 2012). Satellite altimetry measures ice sheet elevation change, computed at orbit crossing points by calculating the difference in ice sheet elevation at a crossover point between ascending and descending satellite passes (e.g. Wingham et al., 1998), using clusters of data points acquired along all ground tracks (e.g. Pritchard et al., 2009), or by differencing height models separated over time (e.g. Csatho et al., 2014). Mass balance is estimated by accounting for changes in bedrock elevation (e.g. Caron and Ivins, 2020) and then by either prescribing the density associated to the elevation fluctuation (e.g. Shepherd et al., 2019) or by making a model-based correction for changes in firn compaction (Sørensen et al., 2011). The technique is unique in charting patterns of mass imbalance with fine (monthly) temporal sampling and fine ( $10^2$  km<sup>2</sup>) spatial resolution, and there are continental-scale measurements dating back to the early 1990s. Satellite measurements of ice velocity computed from sequential radar and optical imagery (e.g. Rignot and Kanagaratnam, 2006) are the basis of ice sheet input-output assessments (e.g. Rignot et al., 2019; Mougnot et al. 2019). Ice velocities are combined with estimates of ice thickness (e.g. Morlighem et al., 2017) to compute changes in marine-terminating glacier discharge, and then with regional climate model estimates of surface mass balance sources (snowfall, rainfall) and sinks (runoff, sublimation, evaporation, and erosion) (e.g. Fettweis et al., 2020; Mottram et al., 2021) to measure temporal changes in net mass balance. The technique provides monthly to annual temporal sampling and drainage basin scale spatial resolution, and there are continental-scale measurements dating back to the late 1970s. During the last decade, new satellite missions with a more frequent revisit time (down to 6 days using image pairs from Sentinel-1a and Sentinel-1b available during the period 2016 to 2021 until the end of Sentinel-1b mission) have been used to improve the temporal resolution of ice velocity measurements, allowing to investigate seasonal fluctuations in ice velocity (King et al., 2018; Lemos et al., 2018) and produce monthly estimates of ice discharge at the continental scale. Mankoff et al. (2021) even produced daily estimates of ice sheet mass balance from the input-output method by resampling the velocity data, however the original temporal resolution of ice velocity measurements does not exceed 12 days. Satellite gravimetry measures fluctuations in Earth's gravitational field, computed using either global spherical harmonic solutions (e.g. Velicogna and Wahr, 2006) or using spatially discrete mass concentration units (e.g. Luthcke et al., 2006). Ice sheet mass changes are determined after making model-based corrections for GIA (e.g. Caron and Ivins, 2020) and for the leakage of mass trends occurring

elsewhere in the climate system, especially those arising from ocean mass variability and changes in land hydrology. The technique provides fine (monthly) temporal sampling and moderate ( $10^5 \text{ km}^2$ ) spatial resolution, dating back to 2002 with the launch of the GRACE mission and the more recent launch of its follow on GRACE-FO in 2018.

## 2.2 Input Data

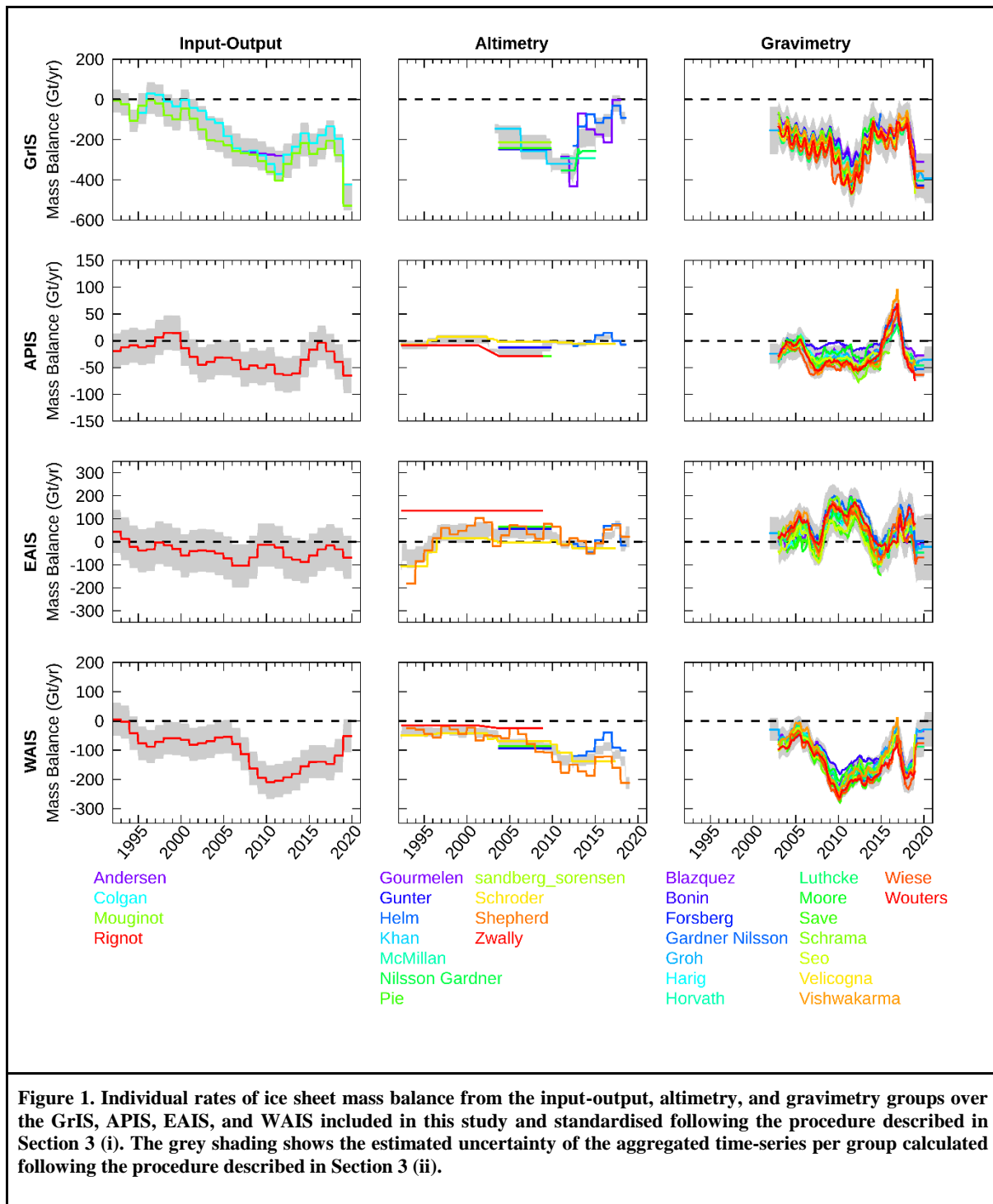
To compile our assessment of Greenland Ice Sheet mass balance we use 27 satellite-based estimates of ice sheet mass change, including 8 estimates based on satellite altimetry, 16 based on satellite gravimetry, and 3 based on the input-output method. Compared to the most recent IMBIE assessment, 12 of these estimates have been updated to include more recent data for Greenland. This set of updated estimates is made of 2 estimates from the input-output method, 1 altimetry estimate, and 9 gravimetry estimates including data from the new GRACE Follow-On space gravimetry mission (GRACE-FO). For our assessment of Antarctica's mass balance, we use 23 satellite-based estimates altogether, with 6 derived from altimetry, 16 from gravimetry, and 1 from the input-output method. More than half of these estimates have been extended in time compared to IMBIE-2. These updated estimates for Antarctica include the input-output method estimate, 2 altimetry estimates, and 10 gravimetry estimates combining GRACE and GRACE-FO data. In total, this new IMBIE assessment includes data from 14 satellite missions, spanning the years 1992 to 2020 – with results from all three geodetic techniques available between 2003 and 2018 in Greenland and 2002 and 2018 in Antarctica – and, for the first time, includes data from the GRACE-FO mission launched in 2018. A wide range of GIA models have been used to correct gravimetric and volumetric mass balance estimates. The models use in this assessment are all forward models, which combine a rheology model of the solid Earth with a model of past ice mass change. In this assessment, only two SMB models have been used in the input-output method estimates included – the RACMO (Regional Atmospheric Climate Model) and MAR (Modèle Atmosphérique Régional) models (Table 1).

<b>Table 1. Synthesis of satellite datasets, GIA, and SMB models used to derive the individual estimates of ice sheet mass balance included in this study. Details and references of the GIA and SMB models are available in Table A1.</b>
--

		1992	1993	1994	1995	1996	1997	1998	1999	2000	2001	2002	2003	2004	2005	2006	2007	2008	2009	2010	2011	2012	2013	2014	2015	2016	2017	2018	2019	2020	
<b>Satellite Missions</b>																															
<b>IOM</b>	ERS-1																														
	ERS-2																														
	RADARSAT-1																														
	ENVISAT																														
	ALOS/PALSAR																														
	RADARSAT-2																														
	TerraSAR-X																														
	COSMO-SkyMed																														
	Landsat-8																														
	Sentinel-1																														
<b>ALT</b>	ERS-1																														
	ERS-2																														
	ENVISAT																														
	ICESat																														
	CryoSat-2																														
<b>GMB</b>	GRACE																														
	GRACE-FO																														
<b>GIA models</b>																															
<b>AIS</b>	A13																														
	A13 and W12a																														
	ICE-5G and W12a																														
	ICE-6G																														
	ICE-6G and A13																														
	ICE-6G and IJ05 R2																														
	IJ05 and W12a																														
	IJ05 R2																														
	IJ05 R2 and A13																														
	IJ05 R2 and Paulson07																														
	IJ05 R2 and Simpson09																														
	IJ05 R2 and W12a																														
	Khan 2016 and W12a																														
	Schrama14																														
W12a																															
<b>GrIS</b>	A13																														
	ICE-5G																														
	ICE-6G																														
	ICE-5G and ICE-6G																														
	ICE-6G and A13																														
	Paulson07																														
	Schrama14																														
	Simpson09																														
<b>SMB models</b>																															
<b>GrIS AIS</b>	RACMO 2.3																														
	MAR 3.2																														
	MAR 3.5.2																														
	RACMO 2.3																														

To achieve a meaningful comparison of ice sheet mass balance estimates, we analyse mass trends using common definitions of the Antarctic, West Antarctic, East Antarctic, Antarctic Peninsula, and Greenland Ice Sheet boundaries (AIS, WAIS, EAIS, APIS, and GrIS, respectively). We use two ice sheet drainage basin sets, both previously used in the past IMBIE assessments (Shepherd et al., 2012; IMBIE Team, 2018; 2020) and available at <http://imbie.org/imbie-3/drainage-basins/>. The first drainage basin set was derived based on ICESat surface elevation data and includes 27 basins in Antarctica covering an area of 11,885,725 km<sup>2</sup> and 19 in Greenland over an area of 1,703,625 km<sup>2</sup> (Zwally et al., 2012) and is retained for consistency with the first IMBIE assessment (Shepherd et al., 2012). The second set defines 18 basins in Antarctica covering 11,892,700 km<sup>2</sup> and 6 in

150 Greenland covering 1,723,300 km<sup>2</sup> (Rignot et al., 2011a; Rignot et al., 2011b). The two ice sheet delineation differ by 1.1 % and 0.1 % of total ice sheet extent for the Greenland and Antarctic Ice Sheets, respectively, and thus using either of these definitions leads to a negligible difference in mass balance (The IMBIE Team, 2018; 2020). IMBIE participants were free to use either of these two definitions, and we combine mass trends over the GrIS, AIS, WAIS, EAIS, and APIS together regardless of what definition was chosen. The different estimates included in this assessment are presented on Figure 1.





## 2.3 Output Data

The output data consists of a single reconciled estimate of ice sheet mass balance covering the period 1<sup>st</sup> January 1992 to 31<sup>st</sup> December 2020 for the GrIS, AIS, APIS, WAIS, EAIS, and the sum of the GrIS and AIS. Two CSV files are provided for each ice sheet region, one with the data provided in Gigatons (Gt) and one with the data provided in equivalent sea level contribution in millimetres (mm). These files contain annual rates of mass balance and cumulative mass changes with their corresponding uncertainties.

## 3 Methods

IMBIE participants contributed time-series of either relative mass change,  $\Delta M(t)$ , or of rate of mass change,  $dM(t)/dt$ , with their associated uncertainty, integrated over at least one of the ice sheet regions defined in the standard drainage basin sets. To produce a reconciled estimate of ice sheet mass change from these individual estimates, we compare and aggregate  $dM(t)/dt$  from each satellite technique. The IMBIE assessment software used to produce the dataset presented in this study is available at <https://doi.org/10.5281/zenodo.7342481>. We apply a consistent processing scheme to all submitted datasets and for all ice sheet regions which consists of: i) computing  $dM(t)/dt$  for all datasets that were submitted as  $\Delta M(t)$ , ii) aggregating time-series of mass trends within each class of satellite observations, iii) combining the altimetry, gravimetry, and input-output time-series to derive a single reconciled time-series of mass trends, and iv) integrating this reconciled time-series of mass trends to produce the final reconciled time-series of cumulative mass change. In what follows, we summarise each of these processing steps:

### 175 *i) Computing time-series of mass trends*

First, we derive time-series of monthly rates of ice sheet mass change,  $dM(t)/dt$ , for all datasets that were submitted as  $\Delta M(t)$  to allow the aggregation of datasets within each satellite observations class as  $dM(t)/dt$  computed using a standardised approach. At each epoch, we estimate  $dM(t)/dt$  by fitting a linear trend to the  $\Delta M(t)$  data falling within a sliding window of 36 months, centred around the given epoch, using a weighted least-squares approach, with each point weighted by its error. The error on the derived time-series is taken as the sum in quadrature of the linear model structural error computed as the standard error of the linear regression  $s_e$  and the mean of the errors of the  $n_w$  points in the original  $\Delta M(t)$  time-series falling within the 36-month sliding window as:

$$\sigma_{\frac{dM}{dt}}(t) = \sqrt{s_e^2 + \left( \frac{1}{n_w} \sum_{i=0}^{n_w-1} \sigma_{\Delta M,i} \right)^2} \quad (1)$$

Finally, the derived time-series of mass trends are truncated by half the window width at the start and end of their period.

### *ii) Aggregating time-series of mass trends from similar satellite observations*

We aggregate the standardised time-series of mass trends within the altimetry, gravimetry, and input-output groups separately to produce three time-series over each ice sheet region  $\left. \frac{dM_{aggr}(t)}{dt} \right|_{group}$ , where *group* refers to

190 one of these three independent satellite techniques (i.e. altimetry, gravimetry, or input-output method). We calculate each aggregated time-series by taking the error-weighted average of the  $n_{estimates\ per\ group}$  individual monthly rates of ice sheet mass change available from the same satellite technique group at each month:

$$\left. \frac{dM_{aggr}(t)}{dt} \right|_{group} = \frac{\sum_{i=0}^{n_{estimates\ per\ group}-1} \left. \frac{dM(t)}{dt} \right|_{group,i} / \sigma_{\left. \frac{dM(t)}{dt} \right|_{group,i}}}{\sum_{i=0}^{n_{estimates\ per\ group}-1} 1 / \sigma_{\left. \frac{dM(t)}{dt} \right|_{group,i}}} \quad (2)$$

The associated error is calculated as the sum in quadrature of the contributing individual time-series errors divided  
195 by the square root of the number of estimates in the group:

$$\sigma_{aggr,group}(t) = \sqrt{\frac{1}{n_{estimates\ per\ group}} \sum_{i=0}^{n_{estimates\ per\ group}-1} \sigma_{\left. \frac{dM(t)}{dt} \right|_{group,i}}^2} \quad (3)$$

iii) *Combining the altimetry, gravimetry, and input-output time-series of mass trends*

We combine the altimetry, gravimetry, and input-output time-series to produce a single reconciled time-series of  
200 mass trends by taking the error-weighted mean of the  $n_{group}$  independent estimates for which a mass trend estimate is available at each epoch (comprised between 1 and 3):

$$\frac{dM_{reconciled}(t)}{dt} = \frac{\sum_{i=0}^{n_{group}-1} \left. \frac{dM_{aggr,i}(t)}{dt} \right| / \sigma_{aggr,i}(t)}{\sum_{i=0}^{n_{group}-1} 1 / \sigma_{aggr,i}(t)} \quad (4)$$

We estimate the error on the reconciled mass trend time-series at each epoch as the sum in quadrature of the aggregated time-series errors divided by the square root of the number of independent estimates available:

$$205 \quad \sigma_{reconciled}(t) = \sqrt{\frac{1}{n_{group}} \sum_{i=0}^{n_{group}-1} \sigma_{aggr,i}^2(t)} \quad (5)$$

Finally, when summing mass trends of multiple ice sheets, the combined uncertainty is estimated as the root sum square of the uncertainties for each region:

$$\sigma_{total}(t) = \sqrt{\sum_{regions} \sigma_{reconciled,i}^2(t)} \quad (6)$$

210 iv) *Generating the final reconciled time-series of cumulative mass change*

We generate a time-series of cumulative ice sheet mass change by integrating our reconciled time-series of mass trends over time for each region. We estimate the cumulative errors as the root sum square of errors, divided by  
12 as our estimates are posted at monthly epochs:

$$\sigma_{cumul}(t) = \sqrt{\frac{1}{12} \sum_{i=0}^{t-1} \sigma_{reconciled}^2(i)} \quad (7)$$

215

Here, we discuss the potential systematic bias introduced by the inclusion of the peripheral glaciers and ice caps (GICs) in the gravimetry estimates included in our assessment as the spatial resolution of satellite gravimetry is not sufficient to resolve separately the mass change signals of these two neighbouring ice masses. To examine this further, we use Hugonnet et al. (2021) dataset (<https://doi.org/10.6096/13>, last access: 23 February 2023), which provides mass balance estimates of the glaciers located at the periphery of the ice sheets derived from high resolution digital elevation models. During the overlap of Hugonnet et al. study and the gravimetry recorded employed in this study (2002-2019), Greenland peripheral glaciers lost mass at a rate of  $35.5 \pm 1.6 \text{ Gt yr}^{-1}$ . In Antarctica (excluding the Sub Antarctic glaciers located further than 1000 km from the ice sheet), peripheral glaciers lost mass at a rate of  $11.8 \pm 3.4 \text{ Gt yr}^{-1}$ ,  $0.7 \pm 1.1 \text{ Gt yr}^{-1}$ , and  $5.7 \pm 2.5 \text{ Gt yr}^{-1}$  at the APIS, EAIS, and WAIS, respectively. To test the impact of the inclusion of the peripheral glaciers in our gravimetry estimates on our reconciled ice sheet mass balance assessment, we use the peripheral glaciers mass trends time-series from Hugonnet et al. to remove the contribution of the GICs on our aggregated gravimetry time-series. We use consecutive 5-year rates of mass change for this analysis and their corresponding uncertainties. For 2020, which is not covered by Hugonnet et al., we use the rate of mass change estimated over the 5-year period 2015-2019 instead. We combine in quadrature the uncertainty on the peripheral GICs mass balance and the uncertainty of our aggregated gravimetry mass balance calculated from Eq. 3. Next, we follow the procedure described in step (iii) to re-combine this modified gravimetry aggregated time-series with the altimetry and input-output aggregated time-series. We compare this modified reconciled estimate to our original estimate and find that removing the contribution of the GICs from the gravimetry time-series results in a reduction in mass loss of 4.1 % and 3.3 % in Greenland and Antarctica, respectively, smaller than the uncertainty bounds of our reconciled estimate (Table A2). This simple analysis shows that the inclusion of the peripheral ice masses in the gravimetry estimates included in this study has a negligible impact on our reconciled mass balance assessment of the WAIS and EAIS, and only a small impact (less than  $10 \text{ Gt yr}^{-1}$ ) on our assessment of the GrIS and APIS.

#### 240 **4 Results**

First, we compare individual estimates of ice sheet mass balance within each of the three geodetic technique experiment groups, separately, to assess the level of agreement among estimates derived using the same technique. Within each group, we compare annual rates of mass change and their standard deviation for each ice sheet region. The input-output group includes significantly fewer mass balance estimates than the other technique experiment groups, but these estimates have the advantage of providing information on the partitioning of mass trends between signals related to SMB and ice dynamics, and they also cover relatively long periods of time (Figure 2). Ice discharge is measured from satellite observations of ice velocities combined with estimates of ice thickness at glaciers' termini, and SMB is derived from regional climate model outputs. To estimate the SMB anomaly in Greenland, two estimates used MAR (version 3.2 and version 3.5.2) and one used RACMO (version 2.3). In Antarctica, the input-output estimate used RACMO (version 2.3). In addition to using different SMB models, those estimates also define different reference periods to calculate the SMB anomalies. All of the mass balance estimates derived in this group were originally posted at annual resolution and we resample them over monthly epochs to aggregate them with estimates from the other groups. We include 3 input-output method estimates of GrIS mass balance, all at annual resolution and that together span the period 1992 to 2020 and overlap during the

255 period 2007 to 2011. During their common period, annual rates of mass change determined from these three input-output datasets have a median difference of 28.5 Gt yr<sup>-1</sup> with a standard deviation of 35 Gt yr<sup>-1</sup>. For Antarctica and its ice sheet components, we include one input-output mass balance estimate which covers the entire 1992 to 2020 period at annual resolution.

260 The altimetry group includes 8 mass balance estimates for the GrIS that together span the years 2003 to 2018, with 4 of these solutions derived from radar altimetry, 2 from laser altimetry, and 2 from a combination of both. We include 6 altimetry mass balance estimates for the AIS which together cover the period 1992 to 2019. In total we include 6 solutions for the EAIS, 6 for the WAIS, and 5 for the APIS. Of these, 2 solutions are derived from radar altimetry, 1 from laser altimetry, and 3 from a combination of both. To derive rates of surface elevation change, various methods were applied to the laser and radar altimetry data including repeat-track, plane fit, or  
265 overlapping footprints techniques. For Greenland, half of the participants corrected the altimetry time-series for the GIA effect while for Antarctica, all participants applied a GIA correction. Next, to derive mass trends from rates of surface elevation change, either a constant density or a spatially and time varying density field from a firn density model forced by a regional climate model, were applied. These solutions have varying temporal resolutions ranging from 1 month to 7.1 yr for an average effective temporal resolution of 3.0 yr for Greenland and 2.6 yr for Antarctica. The temporal resolution of the altimetry group is thus lower than annual, mainly due to  
270 the fact that solutions derived from laser altimetry data were all provided as constant rates spanning the duration of ICESat-1 mission while the radar altimetry solutions have a higher temporal resolution of 0.35 yr for Greenland and 0.47 yr for Antarctica. As there is no overlap period during which all altimetry estimates are available, we compare solutions derived solely from radar altimetry and solutions incorporating laser altimetry data separately.  
275 In Greenland, radar altimetry solutions have a median difference of 144 Gt yr<sup>-1</sup> and standard deviation of 67 Gt yr<sup>-1</sup> during their two-year overlap period (2013 to 2014) while the median difference between laser and combination solutions is 29 Gt yr<sup>-1</sup> with a standard deviation of 29 Gt yr<sup>-1</sup> during their 6-year overlap (2004 to 2009). In Antarctica, the spread between laser solutions is largest at the EAIS with a standard deviation in annual rates of 38 Gt yr<sup>-1</sup> between 2004 and 2008, followed by the WAIS and APIS with standard deviations of 23 Gt yr<sup>-1</sup> and 10 Gt yr<sup>-1</sup>, respectively. On the other hand, radar altimetry solutions show a larger spread at the WAIS (21  
280 Gt yr<sup>-1</sup>) than at the EAIS (14 Gt yr<sup>-1</sup>) during their overlap period (2013 to 2018).

The gravimetry group has the largest number of estimates, with 16 for each ice sheet that together span the period 2002 to 2020. All gravimetry solutions were submitted as time-series of cumulative mass change at monthly resolution resulting in a collective effective resolution of 0.08 yr. All participants submitted estimates for all ice  
285 sheet regions, with 10 participants analysing spherical harmonic gravity field solutions using a wide range of approaches and 6 participants using mass concentration units (usually referred to as mascons) directly estimated from the GRACE and GRACE-FO level-1 K-band ranging data. Various GIA, hydrology leakage, and ocean leakage models were used to correct the gravimetry data for external signals. Overall, there is good agreement between rates of ice sheet mass balance derived from satellite gravimetry. In Greenland, we compare the different  
290 gravimetry solutions over the period 2012 to 2014 and find that annual rates of mass have a median difference of 36 Gt yr<sup>-1</sup>, and standard deviation is 30 Gt yr<sup>-1</sup>. In Antarctica, the different gravimetry solutions overlap over a decade from 2004 to 2014 during which their annual rates of mass balance have a median difference of 41 Gt yr<sup>-1</sup>. When comparing over the different regions of the Antarctic continent, the difference is greatest at the EAIS

with a median difference of 31 Gt yr<sup>-1</sup> and standard deviation of 26 Gt yr<sup>-1</sup>. In the other regions, gravimetry  
295 estimates are in better agreement at the APIS with a median difference of 8 Gt yr<sup>-1</sup> and standard deviation of 10  
Gt yr<sup>-1</sup>, followed by the WAIS where the median difference between estimates reaches 19 Gt yr<sup>-1</sup> and their standard  
deviation is 17 Gt yr<sup>-1</sup>.

Comparing mass balance estimates derived from similar satellite observations reveals that in Greenland, the  
median difference between estimates is the largest for the altimetry group and the smallest for the input-output  
300 group. In Antarctica, the median difference between altimetry estimates is less than 38 Gt yr<sup>-1</sup> and less than 41 Gt  
yr<sup>-1</sup> for gravimetry estimates during their respective overlap periods. However this comparison is limited by the  
varying temporal resolutions of the different datasets – especially for the altimetry group for which constant rates  
of mass change over long periods of time dampen temporal variation in ice sheet mass changes – and by the small  
number of input-output estimates – in particular in Antarctica where only one estimate is available. This limits  
305 our ability to link differences between estimates derived from the same geodetic technique to methodological  
differences, or to the use of different geophysical corrections or auxiliary datasets.

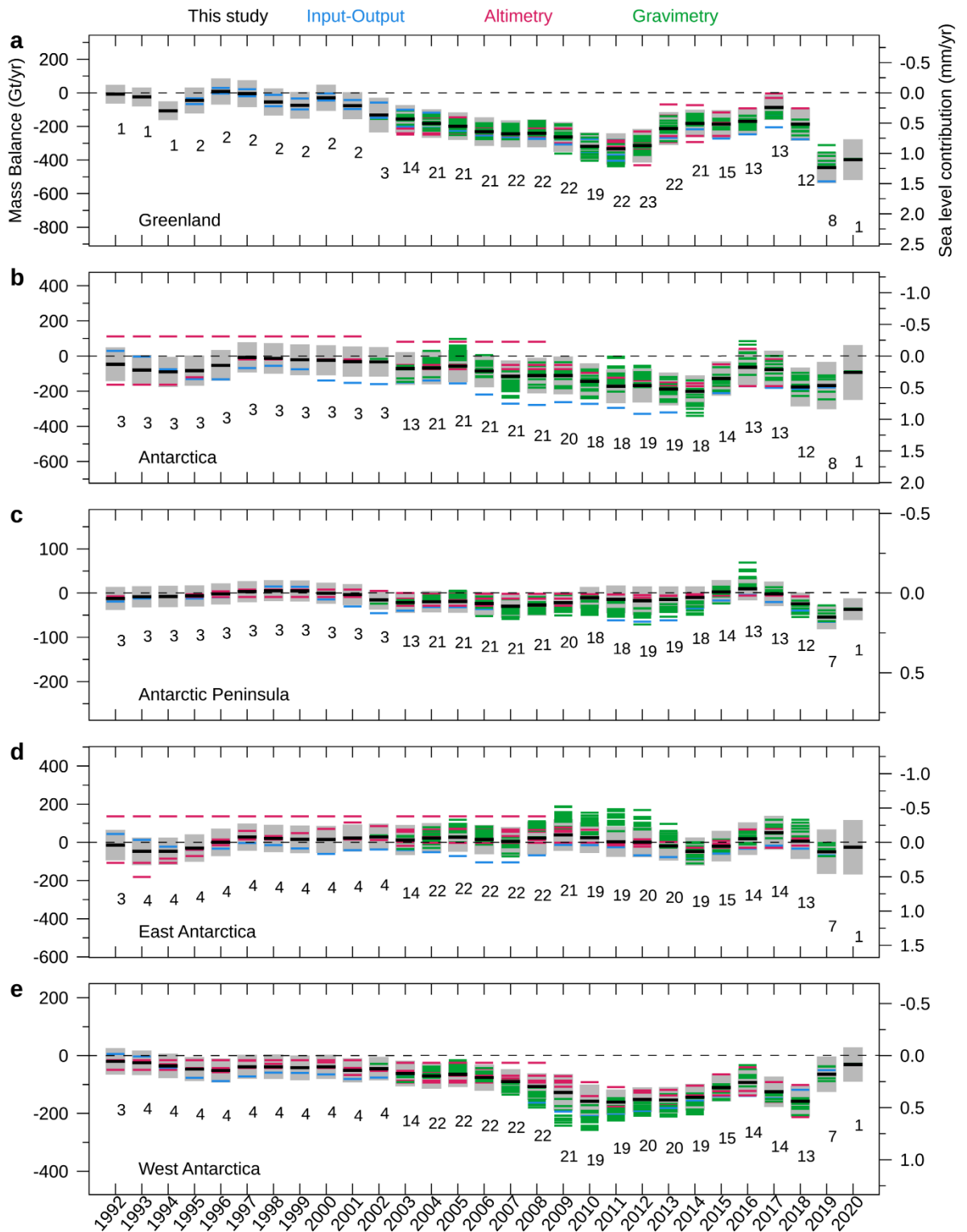


**Figure 2.** Annual rates of mass change of the (a) GrIS, (b) AIS, (c) APIS, (d) EAIS, and (e) WAIS from the altimetry, gravimetry and input-output estimates included in this study (shown by the coloured bars) and the reconciled estimate produced from combining those estimates (shown by the thick black bars). The grey shading shows the uncertainty of our final reconciled estimate, calculated following the procedure described in Section 3 (iii). The number of individual mass balance estimates collated at each epoch is shown below each bar.

Next, we assess differences between the aggregated time-series derived within each class of satellite observations during the periods when estimates from all three geodetic techniques are available – from 2003 to 2018 for Greenland and from 2002 to 2019 for Antarctica (Figure A1). We compare rates of mass change during these overlap periods, which are 5 and 10 years longer than in the previous IMBIE assessments, respectively (Figure 3). We compare the standard deviation in aggregated rates of mass change altimetry, gravimetry and input-output estimates rates of mass change and to the uncertainty of our reconciled mass balance estimate (computed from Eq. 5) to assess whether differences between techniques are significant compared to the uncertainty of our reconciled assessment. In Greenland, rates of mass balance determined from altimetry, gravimetry, and the input-output method are in close agreement between 2003 and 2018, with a standard deviation of 19 Gt yr<sup>-1</sup> and a reconciled rate of mass loss of 221 ± 22 Gt yr<sup>-1</sup> from all three techniques. In Antarctica, the reconciled rate of mass loss between 2003 and 2019 is 115 ± 24 Gt yr<sup>-1</sup> but the spread of the altimetry, gravimetry and input-output estimates is 4 times larger than in Greenland (79 Gt yr<sup>-1</sup>). Over the different regions of Antarctica, the spread of estimates of ice sheet mass balance increases with the size of the region considered, with standard deviations of 54 Gt yr<sup>-1</sup>, 18 Gt yr<sup>-1</sup>, and 16 Gt yr<sup>-1</sup>, at the EAIS, WAIS, and APIS, respectively. Across all ice sheets, the input-output estimate is the most negative and the altimetry the most positive except at the EAIS, where the gravimetry estimate is the most positive. The greatest departure occurs at the EAIS where the three geodetic techniques disagree on even the sign of the mass change, with a maximum difference of 105 ± 33 Gt yr<sup>-1</sup> between rates of mass change from the input-output method and gravimetry estimates. This indicates that the EAIS remains a challenging region for which to monitor mass changes, likely due to the large extent of this region, the poorly constrained GIA signal and paleo-ice reconstruction (Bentley et al., 2014; Martín-Español et al., 2016; Small et al., 2019), and the relatively small mass imbalance in comparison to natural fluctuations in SMB in East Antarctica (Mottram et al., 2021).

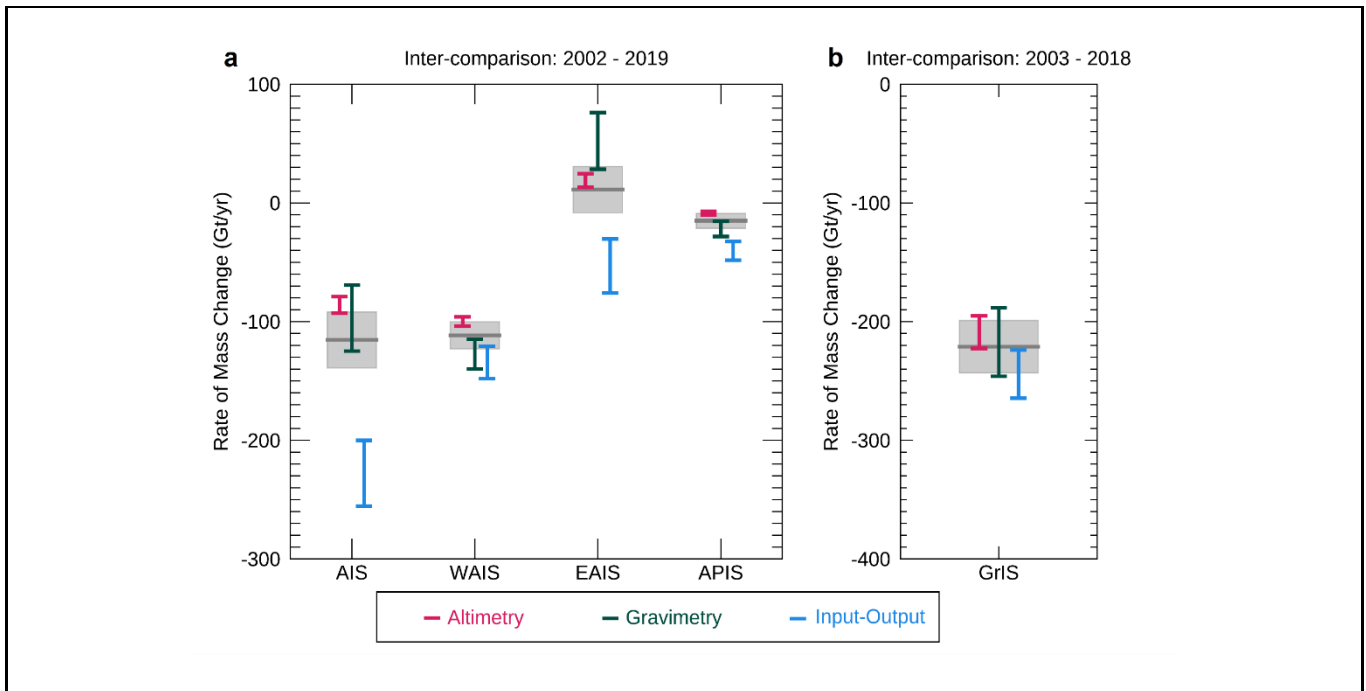


**Figure 3. Inter-comparison of rates of ice sheet mass balance of (a) the AIS, WAIS, EAIS, and APIS over the overlap period 2002-2019 and of (b) the GrIS during the overlap period 2003-2018 derived from the altimetry, gravimetry, and input-output techniques. The coloured bars represent the rates of mass balance and uncertainties of the aggregated technique time-series as calculated in**

**Section 3 step (ii). The grey box represents the rate of mass balance of our final reconciled assessment calculated following the procedure detailed in Section 3 step (iii). The horizontal line in the middle of the box shows the reconciled rate of mass balance and the height of the box represents its associated uncertainty.**

330

When examining the aggregated time-series of rate of mass change at annual resolution, we find the highest temporal correlation between the three time-series at the GrIS ( $0.66 < r^2 < 0.83$ ). In addition, the gravimetry and input-output annual rates are also well-correlated at the APIS and WAIS ( $r^2 = 0.83$ ). However, the altimetry mass balance time-series is poorly correlated with both the aggregated gravimetry and input-output time-series at the APIS and EAIS ( $r^2 < 0.18$ ). The better correlation between the gravimetry and input-output time-series can be explained by their higher temporal resolutions, sufficient to resolve annual fluctuations in ice sheet mass balance which are substantial in these regions. Overall, we find that the vast majority of individual estimates of annual rates of mass balance included in this study fall within the uncertainty bounds of our reconciled estimate given their respective individual errors, with 96 %, 83 %, 83 %, 76 %, and 81 % of those annual rates of mass change falling within the reconciled uncertainty range at the GrIS, AIS, APIS, EAIS, and WAIS, respectively.

335

340

We integrate the combined mass balance estimates from gravimetry, altimetry, and the input-output method (Figure 2) to determine the cumulative mass lost from Antarctica and Greenland since 1992 (Figure 4). Antarctic mass loss continues to be dominated by ice discharge from West Antarctica where the signal is strongest – rising from  $37 \pm 19 \text{ Gt yr}^{-1}$  between 1992 and 1996 to a maximum of  $131 \pm 21 \text{ Gt yr}^{-1}$  between 2012 and 2016 (Table 2), before slowing slightly to  $94 \pm 25 \text{ Gt yr}^{-1}$  during the last 5 years of our survey between 2017 and 2020. At the Antarctic Peninsula the increase in losses since the early 2000s that is generally associated with ice-shelf collapse (Rignot et al., 2004; Cook and Vaughan, 2010; Adusumilli et al., 2018) was masked briefly between 2012 and 2016, when the average rate of mass loss was reduced by  $15 \text{ Gt yr}^{-1}$  to  $6 \pm 13 \text{ Gt yr}^{-1}$  in part due to an extreme snowfall event in 2016 (Wang et al., 2021; Chuter et al., 2021), before returning to  $21 \pm 12 \text{ Gt yr}^{-1}$  between 2017 and 2020. East Antarctica remains the least certain component of Antarctic Ice Sheet mass balance, where the average 30-year mass trend is  $3 \pm 15 \text{ Gt yr}^{-1}$ . In all, the Antarctic Ice Sheet lost  $2671 \pm 530 \text{ Gt}$  of ice between 1992 and 2020, raising the global sea level by  $7.4 \pm 1.5 \text{ mm}$ ; after doubling in the mid-2000s from  $62 \pm 41 \text{ Gt yr}^{-1}$  to  $130 \pm 45 \text{ Gt yr}^{-1}$ , increased Antarctic ice losses – largely driven by an acceleration in ice discharge from the Amundsen Sea Sector (Mouginot et al., 2014) – have persisted to the present-day. The rate of Greenland ice loss has remained highly variable during the last 5-year period of our updated assessment, ranging from  $86 \pm 75 \text{ Gt yr}^{-1}$  in 2017 to a new maximum of  $444 \pm 93 \text{ Gt yr}^{-1}$  in 2019 driven by exceptional surface melting during the summer (Tedesco and Fettweis, 2020). The majority of ice sheet losses have arisen from Greenland during our 29-year survey:  $4892 \pm 457 \text{ Gt}$  in total at an average rate of  $169 \pm 16 \text{ Gt yr}^{-1}$ . Combined, Antarctica and Greenland lost  $7563 \pm 699 \text{ Gt}$  of ice between 1992 and 2020, raising the global sea level by  $21 \pm 2 \text{ mm}$ .

345

350

355



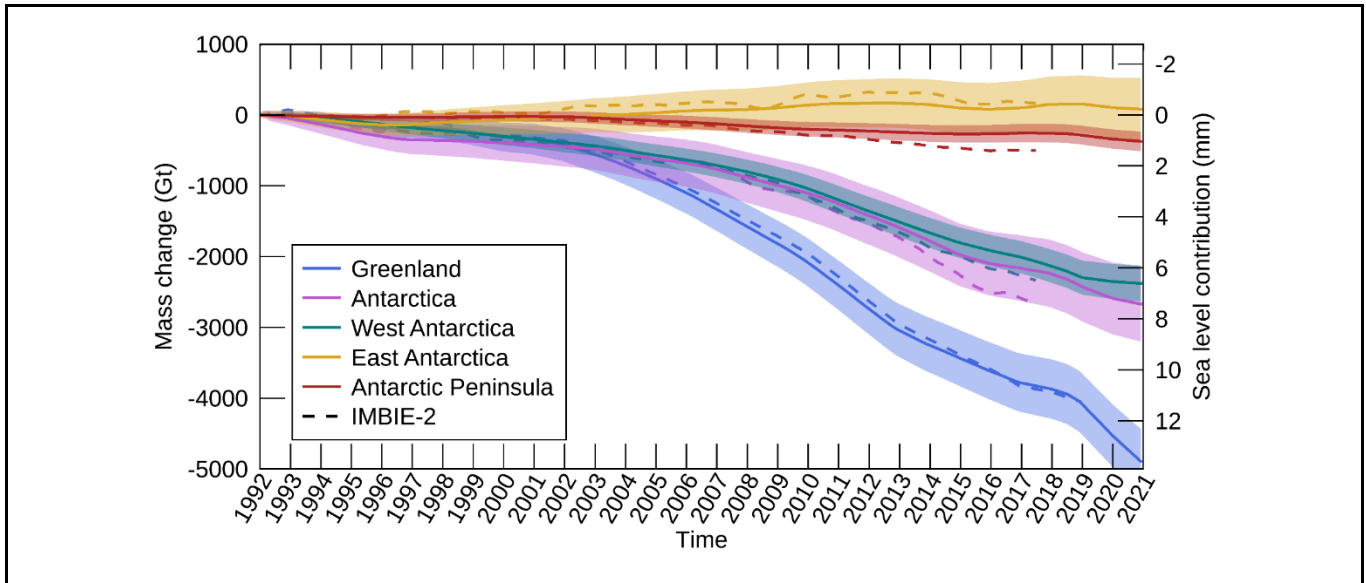


Figure 4. Cumulative ice sheet mass changes. The shadings represent the associated uncertainties and are calculated following the procedure described in Section 3 (iv). The dashed lines show the results from our previous assessments (IMBIE-2).

360

Table 2. Rates of ice sheet mass change ( $\text{Gt yr}^{-1}$ ). Rates are calculated from the first day (1<sup>st</sup> January) of the first year quoted to the last day (31<sup>st</sup> December) of the final year quoted in the table. For context, the last column gives the GMSL trend ( $\text{mm yr}^{-1}$ ), calculated from the AVISO product (<https://www.aviso.altimetry.fr/mssl/>, last access: 12<sup>th</sup> April 2022) over the same period (as the GMSL record starts in 1993, we do not compute the fraction of sea level rise from the ice sheets for the first and last time period of the table).

	GrIS ( $\text{Gt yr}^{-1}$ )	AIS ( $\text{Gt yr}^{-1}$ )	WAIS ( $\text{Gt yr}^{-1}$ )	EAIS ( $\text{Gt yr}^{-1}$ )	APIS ( $\text{Gt yr}^{-1}$ )	GMSL ( $\text{mm yr}^{-1}$ )
<b>1992-1996</b>	$-35 \pm 29$	$-70 \pm 40$	$-37 \pm 19$	$-27 \pm 33$	$-7 \pm 11$	-
<b>1997-2001</b>	$-48 \pm 36$	$-19 \pm 39$	$-42 \pm 19$	$21 \pm 32$	$2 \pm 11$	$3.37 \pm 0.11$
<b>2002-2006</b>	$-180 \pm 39$	$-62 \pm 41$	$-64 \pm 20$	$21 \pm 34$	$-20 \pm 11$	$3.23 \pm 0.06$
<b>2007-2011</b>	$-280 \pm 38$	$-130 \pm 45$	$-129 \pm 23$	$19 \pm 36$	$-21 \pm 12$	$2.44 \pm 0.11$
<b>2012-2016</b>	$-213 \pm 40$	$-150 \pm 43$	$-131 \pm 21$	$-13 \pm 35$	$-6 \pm 13$	$4.96 \pm 0.13$
<b>2017-2020</b>	$-257 \pm 42$	$-115 \pm 55$	$-94 \pm 25$	$0 \pm 47$	$-21 \pm 12$	$4.03 \pm 0.09$
<b>1992-2020</b>	$-169 \pm 16$	$-92 \pm 18$	$-82 \pm 9$	$3 \pm 15$	$-13 \pm 5$	-

## 5 Discussion

### 5.1. Comparison to previous IMBIE assessment

365 Finally, we assess the consistency of our results with our most recent assessment of ice sheet mass balance (IMBIE-2) to evaluate the impact of incorporating updated datasets and using an updated processing scheme. During their overlapping periods – 1992 to 2017 for Antarctica and 1992 to 2018 for Greenland – the results of this study and IMBIE-2 are in agreement within their respective uncertainties with rates of mass change of  $-150.0 \pm 16 \text{ Gt yr}^{-1}$  and  $-150 \pm 12 \text{ Gt yr}^{-1}$  for GrIS, respectively and rates of  $-86 \pm 19 \text{ Gt yr}^{-1}$  and  $-103 \pm 22 \text{ Gt yr}^{-1}$  for AIS, respectively. Next, comparing rates of mass balance within calendar years shows that results from this study and our previous assessment are consistent across all years for all ice sheets, except for two years at the start of our record (1992 and 1995) at the GrIS for which the difference between our mass balance assessments exceeds their respective uncertainty bounds. On average, the magnitude of the differences in annual rates of mass balance is  $36 \text{ Gt yr}^{-1}$  at GrIS,  $33 \text{ Gt yr}^{-1}$  at AIS,  $12 \text{ Gt yr}^{-1}$  at APIS,  $31 \text{ Gt yr}^{-1}$  at EAIS, and  $23 \text{ Gt yr}^{-1}$  at WAIS. The relatively small differences between our previous and current mass balance assessments originate from a combination of our inclusion of updated datasets and the implementation of an updated processing scheme in this study. In all ice sheet regions, participant datasets have been updated compared to our previous assessment. In addition, in this study we apply a common processing scheme to the AIS and GrIS, while in our previous study the mass balance assessments were aggregated with and without inverse-error weighting in the respective regions.

### 380 5.3 Limitations of this study and roadmap for future improvements

In this section, we discuss the limitations of our dataset and a roadmap to improve ice sheet mass balance assessments. The inclusion of the peripheral glaciers and ice caps in the vicinity of the Greenland and Antarctic Ice Sheets is ambiguous in our assessment as not all individual estimates of ice sheet mass balance included here account for those. This relates to the varying ability of satellite techniques to resolve mass balance over those small glaciated areas. Space gravimetry has a coarse spatial resolution of a few hundred kilometres which is not sufficient to separate signals of mass change originating from the ice sheet and its peripheral glaciers. On the other hand, the altimetry estimates included in this assessment exclude the peripheral glaciers and ice caps due to the complex terrain of these glaciers and their relatively small size compared to the footprint size of traditional pulse-limited altimeters. Finally, the input-output estimates do include mass changes from these glaciers, mostly by estimating their changes in SMB. Despite covering a relatively small area (around one tenth of the area of the ice sheets) (Pfeffer et al., 2014), these glaciers contribute significantly to global mean sea level rise with ice losses originating from the Greenland and Antarctic Ice Sheets amounting to  $36 \pm 6 \text{ Gt yr}^{-1}$  and  $21 \pm 5 \text{ Gt yr}^{-1}$  during the period 2010-2019, respectively (Hugonnet et al., 2021). In addition, ice losses have accelerated in the periphery of the Greenland Ice Sheet, with glacier mass loss increasing by 64 % between 2003-2009 and 2018-2021 (Khan et al., 2022). These glaciers therefore need to be accounted for without ambiguity in future IMBIE assessments to remove systematic biases between the different satellite techniques linked to their (non-)inclusion in individual mass balance estimates. Here, we performed a simple analysis to assess the potential impact of the ambiguous inclusion of these peripheral ice masses in our reconciled mass balance assessment and showed that this impact is limited thanks to the fact that we are aggregating different satellite techniques together – including some able to resolve separately ice sheet mass changes – and a different weighting has been applied to the different estimates included. However, future approaches to address this issue will require careful treatment of the leakage of mass

signals between the ice sheets and their peripheral GICs within the gravimetry community, rather than being limited to a subsequent removal of the contribution of these glaciers as we have done here. This will nonetheless require robust mass balance estimates for developing and evaluating new methods. The recent inventory of Earth's  
405 glaciers from satellite photogrammetry (Hugonnet et al., 2021), recent progress in satellite altimetry – with the development of CryoSat-2 swath radar altimetry for measuring mass changes of mountain glaciers (Foresta et al., 2016; Jakob et al., 2021) and the launch of ICESat-2 –, and new community initiatives, such as GlambIE (the Glacier mass balance Inter-comparison Exercise), will further contribute to this effort.

Continuing efforts to understand the remaining differences between altimetry, gravimetry, and the input-output  
410 method is critical to provide more robust observational estimates of the contribution of the ice sheets to GMSL. Producing estimates with a better temporal resolution by using data from the newest satellite missions, reprocessing the satellite record with the newest geophysical corrections, and using a better uncertainty characterisation, will undoubtedly help further reconcile satellite assessments of ice sheet mass balance produced from different techniques. To achieve this, it is also important to assess the impact of SMB and GIA models. SMB  
415 processes are responsible for a large proportion of Greenland's ice losses (and to a lesser extent of Antarctica's ice losses) (Enderlin et al., 2014; Shepherd et al., 2020), and thus pursuing the efforts of recent model inter-comparisons (Fettweis et al., 2020; Mottram et al., 2021) is key to improve the agreement between input-output estimates but also to partition mass trends into SMB and ice dynamics components as it provides critical information on the dominant processes at play. A model-inter-comparison of GIA models would also be timely  
420 as new approaches have been developed in recent years to determine the GIA signal (Whitehouse, 2018). New data-driven solutions that rely on present day geodetic observations (e.g. Riva et al., 2009; Vishwakarma et al., 2022), and solutions derived from coupling a GIA model to an ice sheet mode (de Boer et al., 2017) have become available. Examining the variability of GIA solutions determined from forward models, data inversion, and coupled models will help reducing uncertainties in space gravimetry estimates of ice sheet mass balance.

425 Finally, improving the spatial resolution of the IMBIE assessment by producing time-series of mass changes within the individual basins of the Greenland and Antarctic Ice Sheets will also contribute to further identify areas of similarities and disagreement between satellite techniques (Sutterley et al., 2014) and will support the identification of spatial biases in satellite estimates of ice sheet mass balance. In addition, regional assessments of ice sheet mass balance could support the evaluation and calibration of ice sheet models, contributing to reducing  
430 uncertainties in future sea level rise projections (Edwards et al., 2021; Nias et al., 2019).

## 6 Conclusions

We combine 50 estimates of ice sheet mass balance, 27 for Greenland and 23 for Antarctica, to produce a new reconciled estimate of ice sheet mass balance showing that the ice sheets lost  $7,563 \pm 699$  Gt of ice between 1992 and 2020. Ice losses have accelerated at both ice sheets over this 29-year record and the rate of ice loss is now 5  
435 times higher in Greenland and 25 % higher in Antarctica compared to the early 1990s. Our assessment shows that the altimetry, gravimetry, and input-output method are in close agreement in Greenland with a spread of  $19 \text{ Gt yr}^{-1}$  over their common time period, which represents only 10.9 % of the rate of imbalance. In Antarctica, the spread between techniques is 4 times larger than in Greenland, mostly due to large differences between estimates for the

440 East Antarctic Ice Sheet. To further explore and interpret differences between geodetic techniques, producing  
altimetry estimates with a higher temporal resolution (especially during the first half of the satellite altimetry  
record), better GIA constraints for the gravimetry estimates, and additional estimates of ice sheet mass balance  
via the input-output method would improve the comparison and aggregation of ice sheet mass balance estimates.  
Continuously monitoring the mass balance of the ice sheets and producing annual updates of Greenland and  
Antarctica mass balance is critical to track their contribution to global mean sea level and constrain projections of  
445 future sea-level rise.

## 7 Data Availability

The aggregated Greenland and Antarctic Ice Sheets mass balance data and associated errors generated in this  
study are freely available at the NERC Polar Data Centre, <https://doi.org/10.5285/77B64C55-7166-4A06-9DEF-2E400398E452> (The IMBIE Team, 2021).

## 450 8 Code Availability

The code used to compute and aggregate rates of ice sheet mass change and their errors is freely available at  
<https://github.com/IMBIE>.

## Author Contribution

The executive committee of IMBIE (A.S., E.R.I., N.J.S., I.N.O, C.A., M.B., M.H., I.J., M.D.K., G.K., S.N.,  
455 A.J.P., E.R., T.S., K.M.S., B.E.S., L.S.S., I.V., P.L.W.) designed the study. A.S., L.S.S., A.G., L.G., N.G., B.C.G.,  
V.H., S.A.K, H.K., M.M, J.N., N.P., L.S., and S.B.S. contributed altimetry estimates. M.H., I.V., A.B., R.F., A.G.,  
A. Groh, C.H., C.L., B.D.L., J.N., I.S., H.V.S., K.S., E.J.O.S., T.C.S., B.D.V, D.W., and B.W contributed  
gravimetry estimates. E.R., A.P.A., W.C., J.M., and B.S. contributed input-output estimates. M.B., C.Agosta,  
X.F., H.G., C.K., P.L.L., S.H.M., R.M., and B.N. contributed SMB estimates. G.A., B.S.L, D.M., W.R.P, G.S.,  
460 M.W., and W.W. contributed GIA estimates. I.N.O. and M.E.P. performed the mass balance data collation. I.N.O.  
prepared the datasets comparison. I.N.O. led the writing and prepared the other figures and tables. I.N.O, A.S. and  
T. Slater wrote the manuscript. All authors participated in the data interpretation and commented on the  
manuscript.

## Competing interests

465 C. A. is member of the editorial board of journal Earth System Science Data.

## Acknowledgements

This work is an outcome of the Ice Sheet Mass Balance Inter-comparison Exercise (IMBIE) supported by the ESA  
EOEP-5 ‘EO Science for Society’, the ESA ‘Climate Change Initiative’, and the NASA Cryosphere Program. A  
portion of this research was carried out at the Jet Propulsion Laboratory, California Institute of Technology, under  
470 a contract with the National Aeronautics and Space Administration (NASA) (80NM0018D0004). Funding for E.I.

and N-J.S. was provided by NASA ROSES solicitation NNH20ZDA001N-CRYO in response to Proposal 20-CRYO2020-0003. GEUS data provided from the Programme for Monitoring of the Greenland Ice Sheet (www.PROMICE.dk) was funded by the Danish Ministry of Climate, Energy and Utilities. M.M. acknowledges the support of the UK NERC Centre for Polar Observation and Modelling (CPOM), and the Lancaster University-  
475 UKCEH Centre of Excellence in Environmental Data Science. P. L. L. gratefully acknowledges the contributions of Aarhus University Interdisciplinary Centre for Climate Change (iClimate, Aarhus University). N.G. used CryoSat data obtained from ESA at [cs2eo.org](https://cs2eo.org) and via the CryoTEMPO-EOLIS project <https://cryotempo-eolis.org/>. G.S. is funded by a research grant of DIFA (Dipartimento di Fisica e Astronomia “Augusto Righi”) of the Alma Mater Studiorum Università di Bologna. J.N. and A.G. were supported by the ITS\_LIVE project  
480 awarded through NASA MEaSUREs program, and the NASA Cryosphere program through participation in the ICESat-2 science team. I.S. acknowledges funding by the Helmholtz Climate Initiative REKLIM (Regional Climate Change), a joint research project of the Helmholtz Association of German Research Centres (HGF). Ice velocity data for Greenland and Antarctica provided by UC Irvine is funded by NASA MEaSUREs program.  
485 BedMachine Antarctica is funded by NASA MEaSUREs program. BedMachine Greenland is funded by research grants from NASA Operation IceBridge Mission. BW was funded by NWO VIDI grant 016.Vidi.171.063.

## 490 References

- Adusumilli, S., Fricker, H. A., Medley, B., Padman, L., and Siegfried, M. B.: Interannual variations in meltwater input to the Southern Ocean from Antarctic ice shelves, *Nat. Geosci.*, 13, 616–620, <https://doi.org/10.1038/s41561-020-0616-z>, 2020.
- 495 Adusumilli, S., Fricker, H. A., Siegfried, M. R., Padman, L., Paolo, F. S., and Ligtenberg, S. R. M.: Variable Basal Melt Rates of Antarctic Peninsula Ice Shelves, 1994–2016, *Geophysical Research Letters*, 45, 4086–4095, <https://doi.org/10.1002/2017GL076652>, 2018.
- Aschwanden, A., Bartholomaus, T. C., Brinkerhoff, D. J., and Truffer, M.: Brief communication: A roadmap  
500 towards credible projections of ice sheet contribution to sea level, *The Cryosphere*, 15, 5705–5715, <https://doi.org/10.5194/tc-15-5705-2021>, 2021.
- Bentley, M. J., Ó Cofaigh, C., Anderson, J. B., Conway, H., Davies, B., Graham, A. G. C., Hillenbrand, C.-D., Hodgson, D. A., Jamieson, S. S. R., Larter, R. D., Mackintosh, A., Smith, J. A., Verleyen, E., Ackert, R. P., Bart, P. J., Berg, S., Brunstein, D., Canals, M., Colhoun, E. A., Crosta, X., Dickens, W. A., Domack, E., Dowdeswell, J. A., Dunbar, R., Ehrmann, W., Evans, J., Favier, V., Fink, D., Fogwill, C. J., Glasser, N. F., Gohl, K., Gollledge, N. R., Goodwin, I., Gore, D. B., Greenwood, S. L., Hall, B. L., Hall, K., Hedding, D. W., Hein, A. S., Hocking, E. P., Jakobsson, M., Johnson, J. S., Jomelli, V., Jones, R. S., Klages, J. P., Kristoffersen, Y., Kuhn, G., Leventer, A., Licht, K., Lilly, K., Lindow, J., Livingstone, S. J., Massé, G., McGlone, M. S., McKay, R. M., Melles, M.,

- 510 Miura, H., Mulvaney, R., Nel, W., Nitsche, F. O., O'Brien, P. E., Post, A. L., Roberts, S. J., Saunders, K. M.,  
Selkirk, P. M., Simms, A. R., Spiegel, C., Stollendorf, T. D., Sugden, D. E., van der Putten, N., van Ommen, T.,  
Verfaillie, D., Vyverman, W., Wagner, B., White, D. A., Witus, A. E., and Zwartz, D.: A community-based  
geological reconstruction of Antarctic Ice Sheet deglaciation since the Last Glacial Maximum, *Quaternary Science  
Reviews*, 100, 1-9, 2014.
- 515 Caron, L. and Ivins, E. R.: A baseline Antarctic GIA correction for space gravimetry, *Earth and Planetary Science  
Letters*, 531, 115957, <https://doi.org/10.1016/j.epsl.2019.115957>, 2020.
- 520 Church, J. A., Clark, P. U., Cazenave, A., Gregory, J. M., Jevrejeva, S., Levermann, A., Merrifield, M. A., Milne,  
G. A., Nerem, R. S., Nunn, P. D., Payne, A. J., Pfeffer, W. T., Stammer, D., and Unnikrishnan, A. S.: Sea Level  
Change, in: *Climate Change 2013: The Physical Science Basis. Contribution of Working Group I to the Fifth  
Assessment Report of the Intergovernmental Panel on Climate Change*, edited by: Stocker, T. F., Qin, D., Plattner,  
G.-K., Tignor, M., Allen, S. K., Boschung, J., Nauels, A., Xia, Y., Bex, V., and Midgley, P. M., Cambridge  
University Press, Cambridge, United Kingdom and New York, NY, USA, 1137–1216,  
<https://doi.org/10.1017/CBO9781107415324.026>, 2013.
- 525 Chuter, S. J., Zammit-Mangion, A., Rougier, J., Dawson, G., and Bamber, J. L.: Mass evolution of the Antarctic  
Peninsula over the last two decades from a joint Bayesian inversion, *The Cryosphere*, 1–32,  
<https://doi.org/10.5194/tc-2021-178>, 2021.
- 530 Cook, A. J. and Vaughan, D. G.: Overview of areal changes of the ice shelves on the Antarctic Peninsula over the  
past 50 years, *The Cryosphere*, 4, 77–98, <https://doi.org/10.5194/tc-4-77-2010>, 2010.
- 535 Csatho, B. M., Schenk, A. F., van der Veen, C. J., Babonis, G., Duncan, K., Rezvanbehbahani, S., van den Broeke,  
M. R., Simonsen, S. B., Nagarajan, S., and van Angelen, J. H.: Laser altimetry reveals complex pattern of  
Greenland Ice Sheet dynamics, *Proceedings of the National Academy of Sciences of the United States of America*,  
111, 18478-18424, 2014.
- 540 de Boer, B., Stocchi, P., Whitehouse, P. L., and van de Wal, R. S. W.: Current state and future perspectives on  
coupled ice-sheet – sea-level modelling, *Quaternary Science Reviews*, 169, 13-28,  
<https://doi.org/10.1016/j.quascirev.2017.05.013>, 2017.
- 545 Edwards, T. L., Nowicki, S., Marzeion, B., Hock, R., Goelzer, H., Seroussi, H., Jourdain, N. C., Slater, D. A.,  
Turner, F. E., Smith, C. J., McKenna, C. M., Simon, E., Abe-Ouchi, A., Gregory, J. M., Larour, E., Lipscomb, W.  
H., Payne, A. J., Shepherd, A., Agosta, C., Alexander, P., Albrecht, T., Anderson, B., Asay-Davis, X.,  
Aschwanden, A., Barthel, A., Bliss, A., Calov, R., Chambers, C., Champollion, N., Choi, Y., Cullather, R.,  
Cuzzone, J., Dumas, C., Felikson, D., Fettweis, X., Fujita, K., Galton-Fenzi, B. K., Gladstone, R., Gолledge, N.  
R., Greve, R., Hattermann, T., Hoffman, M. J., Humbert, A., Huss, M., Huybrechts, P., Immerzeel, W., Kleiner,  
T., Kraaijenbrink, P., Le Clec'h, S., Lee, V., Leguy, G. R., Little, C. M., Lowry, D. P., Malles, J.-H., Martin, D.  
F., Maussion, F., Morlighem, M., O'Neill, J. F., Nias, I., Pattyn, F., Pelle, T., Price, S. F., Quiquet, A., Radić, V.,  
Reese, R., Rounce, D. R., Rückamp, M., Sakai, A., Shafer, C., Schlegel, N.-J., Shannon, S., Smith, R. S., Straneo,

- F., Sun, S., Tarasov, L., Trusel, L. D., Van Breedam, J., van de Wal, R., van den Broeke, M., Winkelmann, R., Zekollari, H., Zhao, C., Zhang, T., and Zwinger, T.: Projected land ice contributions to twenty-first-century sea level rise, *Nature*, 593, 74–82, <https://doi.org/10.1038/s41586-021-03302-y>, 2021.
- 550
- Enderlin, E. M., Howat, I. M., Jeong, S., Noh, M. J., Angelen, J. H., and Broeke, M. R.: An improved mass budget for the Greenland ice sheet, *Geophysical Research Letters*, 41, 866–872, <https://doi.org/10.1002/2013GL059010>, 2014.
- 555
- Fettweis, X., Hofer, S., Krebs-Kanzow, U., Amory, C., Aoki, T., Berends, C. J., Born, A., Box, J. E., Delhasse, A., Fujita, K., Gierz, P., Goelzer, H., Hanna, E., Hashimoto, A., Huybrechts, P., Kapsch, M.-L., King, M. D., Kittel, C., Lang, C., Langen, P. L., Lenaerts, J. T. M., Liston, G. E., Lohmann, G., Mernild, S. H., Mikolajewicz, U., Modali, K., Mottram, R. H., Niwano, M., Noël, B., Ryan, J. C., Smith, A., Streffing, J., Tedesco, M., van de Berg, W. J., van den Broeke, M., van de Wal, R. S. W., van Kampenhout, L., Wilton, D., Wouters, B., Ziemen, F., and Zolles, T.: GrSMBMIP: intercomparison of the modelled 1980–2012 surface mass balance over the Greenland Ice Sheet, *The Cryosphere*, 14, 3935–3958, <https://doi.org/10.5194/tc-14-3935-2020>, 2020.
- 560
- Foresta, L., Gourmelen, N., Pálsson, F., Nienow, P., Björnsson, H., and Shepherd, A.: Surface elevation change and mass balance of Icelandic ice caps derived from swath mode CryoSat-2 altimetry, *Geophysical Research Letters*, 43(12), 138–12, <https://doi.org/10.1002/2016GL071485>, 2016.
- 565
- Fox-Kemper, B., Hewitt, H. T., Xiao, C., Aðalgeirsdóttir, G., Drijfhout, S. S., Edwards, T. L., Golledge, N. R., Hemer, M., Kopp, R. E., Krinner, G., Mix, A., Notz, D., Nowicki, S., Nurhati, I. S., Ruiz, L., Sallée, J.-B., Slangen, A. B. A., and Yu, Y.: *Ocean, Cryosphere and Sea Level Change*, Cambridge University Press, 2021.
- Gardner, A. S., Moholdt, G., Scambos, T., Fahnestock, M., Ligtenberg, S., van den Broeke, M., and Nilsson, J.: Increased West Antarctic and unchanged East Antarctic ice discharge over the last 7 years, *The Cryosphere*, 12, 521–547, <https://doi.org/10.5194/tc-12-521-2018>, 2018.
- 570
- Groh, A. and Horwath, M.: Antarctic Ice Mass Change Products from GRACE/GRACE-FO Using Tailored Sensitivity Kernels, *Remote Sensing*, 13, 1736, <https://doi.org/10.3390/rs13091736>, 2021.
- 575
- Hanna, E., Cappelen, J., Fettweis, X., Mernild, S. H., Mote, T. L., Mottram, R., Steffen, K., Ballinger, T. J., and Hall, R. J.: Greenland surface air temperature changes from 1981 to 2019 and implications for ice-sheet melt and mass-balance change, *International Journal of Climatology*, 41, E1336–E1352, <https://doi.org/10.1002/joc.6771>, 2021.
- 580
- Hanson, S., Nicholls, R., Ranger, N., Hallegatte, S., Corfee-Morlot, J., Herweijer, C., and Chateau, J.: A global ranking of port cities with high exposure to climate extremes, *Climatic Change*, 104, 89–111, <https://doi.org/10.1007/s10584-010-9977-4>, 2011.
- 585
- Hofer, S., Tedstone, A. J., Fettweis, X., and Bamber, J. L.: Decreasing cloud cover drives the recent mass loss on

- the Greenland Ice Sheet, *Science*, 3, e1700584–e1700584, <https://doi.org/10.1126/sciadv.1700584>, 2017.
- 590 Hogg, A. E., Shepherd, A., Cornford, S. L., Briggs, K. H., Gourmelen, N., Graham, J. A., Joughin, I., Mouginot, J., Nagler, T., Payne, A. J., Rignot, E., and Wuite, J.: Increased ice flow in Western Palmer Land linked to ocean melting, *Geophysical Research Letters*, 44, 4159–4167, <https://doi.org/10.1002/2016GL072110>, 2017.
- Hugonnet, R., McNabb, R., Berthier, E., Menounos, B., Nuth, C., Girod, L., Farinotti, D., Huss, M., Dussailant, I., Brun, F., and Käab, A.: Accelerated global glacier mass loss in the early twenty-first century, *Nature*, 592, 726–731, <https://doi.org/10.1038/s41586-021-03436-z>, 2021.
- 595 IMBIE Team: Mass balance of the Antarctic Ice Sheet from 1992 to 2017, *Nature*, 558, 219–222, <https://doi.org/10.1038/s41586-018-0179-y>, 2018.
- IMBIE Team: Mass balance of the Greenland Ice Sheet from 1992 to 2018, *Nature*, 579, 233–239, <https://doi.org/10.1038/s41586-019-1855-2>, 2020.
- 600 IMBIE Team: Antarctic and Greenland Ice Sheet mass balance 1992–2020 for IPCC AR6 (Version 1.0) [Data set]. UK Polar Data Centre, Natural Environment Research Council, UK Research & Innovation, available at: <https://doi.org/10.5285/77B64C55-7166-4A06-9DEF-2E400398E452>, 2021.
- 605 Jakob, L., Gourmelen, N., Ewart, M., and Plummer, S.: Spatially and temporally resolved ice loss in High Mountain Asia and the Gulf of Alaska observed by CryoSat-2 swath altimetry between 2010 and 2019, *The Cryosphere*, 15, 1845–1862, <https://10.5194/tc-15-1845-2021>, 2021.
- Jenkins, A., Shoosmith, D., Dutrieux, P., Jacobs, S., Kim, T. W., Lee, S. H., Ha, H. K., and Stammerjohn, S.: 610 West Antarctic Ice Sheet retreat in the Amundsen Sea driven by decadal oceanic variability, *Nature Geosci*, 11, 733–738, <https://doi.org/10.1038/s41561-018-0207-4>, 2018.
- Joughin, I., Shapero, D., Smith, B., Dutrieux, P., and Barham, M.: Ice-shelf retreat drives recent Pine Island Glacier speedup, *Science*, 7, eabg3080, <https://doi.org/10.1126/sciadv.abg3080>, 2021.
- 615 Khan, S. A., Colgan, W., Neumann, T. A., van den Broeke, M. R., Brunt, K. M., Noël, B., Bamber, J. L., Hassan, J., and Björk, A. A.: Accelerating Ice Loss From Peripheral Glaciers in North Greenland, *Geophysical Research Letters*, 49, e2022GL098915, <https://doi.org/10.1029/2022GL098915>, 2022.
- 620 King, M. D., Howat, I. M., Jeong, S., Noh, M. J., Wouters, B., Noël, B., and van den Broeke, M. R.: Seasonal to decadal variability in ice discharge from the Greenland Ice Sheet, *The Cryosphere*, 12, 3813, <https://doi.org/10.5194/tc-12-3813-2018>, 2018.
- 625 King, M. D., Howat, I. M., Candela, S. G., Noh, M. J., Jeong, S., Noël, B. P. Y., van den Broeke, M. R., Wouters, B., and Negrete, A.: Dynamic ice loss from the Greenland Ice Sheet driven by sustained glacier retreat,



Communications Earth & Environment, 1, 1–7, <https://doi.org/10.1038/s43247-020-0001-2>, 2020.

630 Konrad, H., Gilbert, L., Cornford, S. L., Payne, A., Hogg, A., Muir, A., and Shepherd, A.: Uneven onset and pace of ice-dynamical imbalance in the Amundsen Sea Embayment, West Antarctica, *Geophysical Research Letters*, 44, 910–918, <https://doi.org/10.1002/2016GL070733>, 2017.

Konrad, H., Shepherd, A., Gilbert, L., Hogg, A. E., McMillan, M., Muir, A., and Slater, T.: Net retreat of Antarctic glacier grounding lines, *Nature Geosci*, 11, 258–262, <https://doi.org/10.1038/s41561-018-0082-z>, 2018.

635 Kulp, S. A. and Strauss, B. H.: New elevation data triple estimates of global vulnerability to sea-level rise and coastal flooding, *Nat Commun*, 10, 1–12, <https://doi.org/10.1038/s41467-019-12808-z>, 2019.

640 Leeson, A. A., Shepherd, A., Briggs, K., Howat, I., Fettweis, X., Morlighem, M., and Rignot, E.: Supraglacial lakes on the Greenland ice sheet advance inland under warming climate, *Nature Climate Change*, 5, 51–55, <https://doi.org/10.1038/nclimate2463>, 2015.

Lemos, A., Shepherd, A., McMillan, M., and Hogg, A. E.: Seasonal Variations in the Flow of Land-Terminating Glaciers in Central-West Greenland Using Sentinel-1 Imagery, *Remote Sensing*, 10, 1878, <https://doi.org/10.3390/rs10121878>, 2018.

645

Luthcke, S. B., Zwally, H. J., Abdalati, W., Rowlands, D. D., Ray, R. D., Nerem, R. S., Lemoine, F. G., McCarthy, J. J., and Chinn, D. S.: Recent Greenland Ice Mass Loss by Drainage System from Satellite Gravity Observations, *Science*, 314, 1286–1289, <https://doi.org/10.1126/science.1130776>, 2006.

650 Mankoff, K. D., Fettweis, X., Langen, P. L., Stendel, M., Kjeldsen, K. K., Karlsson, N. B., Noël, B., van den Broeke, M. R., Solgaard, A., Colgan, W., Box, J. E., Simonsen, S. B., King, M. D., Ahlstrøm, A. P., Andersen, S. B., and Fausto, R. S.: Greenland ice sheet mass balance from 1840 through next week, *Earth Syst. Sci. Data*, 13, 5001–5025, <https://doi.org/10.5194/essd-13-5001-2021>, 2021.

655 Martín-Español, A., King, M. A., Zammit-Mangion, A., Andrews, S. B., Moore, P., and Bamber, J. L.: An assessment of forward and inverse GIA solutions for Antarctica, *Journal of geophysical research. Solid earth*, 121, 6947–6965, <https://doi.org/10.1002/2016JB013154>, 2016.

660 Milillo, P., Rignot, E., Rizzoli, P., Scheuchl, B., Mouginot, J., Bueso-Bello, J. L., Prats-Iraola, P., and Dini, L.: Rapid glacier retreat rates observed in West Antarctica, *Nat. Geosci.*, 1–6, <https://doi.org/10.1038/s41561-021-00877-z>, 2022.

Moon, T., Joughin, I., Smith, B., and Howat, I.: 21st-Century Evolution of Greenland Outlet Glacier Velocities, *Science*, 336, 576–578, <https://doi.org/10.1126/science.1219985>, 2012.

- 665 Morlighem, M., Williams, C. N., Rignot, E., An, L., Arndt, J. E., Bamber, J. L., Catania, G., Chauché, N.,  
Dowdeswell, J. A., Dorschel, B., Fenty, I., Hogan, K., Howat, I., Hubbard, A., Jakobsson, M., Jordan, T. M.,  
Kjeldsen, K. K., Millan, R., Mayer, L., Mouginot, J., Noël, B. P. Y., O’Cofaigh, C., Palmer, S., Rysgaard, S.,  
Seroussi, H., Siegert, M. J., Slabon, P., Straneo, F., van den Broeke, M. R., Weinrebe, W., Wood, M., and  
Zinglensen, K. B.: BedMachine v3: Complete Bed Topography and Ocean Bathymetry Mapping of Greenland  
670 From Multibeam Echo Sounding Combined With Mass Conservation, *Geophysical Research Letters*, 44, 11,051-  
011,061, <https://doi.org/10.1002/2017GL074954>, 2017.
- Mottram, R., Hansen, N., Kittel, C., van Wessem, J. M., Agosta, C., Amory, C., Boberg, F., van de Berg, W. J.,  
Fettweis, X., Gossart, A., van Lipzig, N. P. M., van Meijgaard, E., Orr, A., Phillips, T., Webster, S., Simonsen, S.  
B., and Souverijns, N.: What is the surface mass balance of Antarctica? An intercomparison of regional climate  
model estimates, *The Cryosphere*, 15, 3751–3784, <https://doi.org/10.5194/tc-15-3751-2021>, 2021.
- 675 Mouginot, J., Rignot, E., and Scheuchl, B.: Sustained increase in ice discharge from the Amundsen Sea  
Embayment, West Antarctica, from 1973 to 2013, *Geophysical Research Letters*, 41, 1576–1584,  
<https://doi.org/10.1002/2013GL059069>, 2014.
- Mouginot, J., Rignot, E., Scheuchl, B., and Millan, R.: Comprehensive Annual Ice Sheet Velocity Mapping Using  
680 Landsat-8, Sentinel-1, and RADARSAT-2 Data, *Remote Sensing*, 9, 364, <https://doi.org/10.3390/rs9040364>,  
2017.
- Mouginot, J., Rignot, E., Bjørk, A. A., van den Broeke, M., Millan, R., Morlighem, M., Noël, B., Scheuchl, B.,  
and Wood, M.: Forty-six years of Greenland Ice Sheet mass balance from 1972 to 2018, *Proceedings of the*  
685 *National Academy of Sciences*, 116, 9239-9244, <https://doi.org/10.1073/pnas.1904242116>, 2019.
- Nias, I. J., Cornford, S. L., Edwards, T. L., Gourmelen, N., and Payne, A. J.: Assessing Uncertainty in the  
Dynamical Ice Response to Ocean Warming in the Amundsen Sea Embayment, West Antarctica, *Geophysical*  
*Research Letters*, 46, 11253-11260, <https://doi.org/10.1029/2019GL084941>, 2019.
- 690 Paolo, F. S., Fricker, H. A., and Padman, L.: Volume loss from Antarctic ice shelves is accelerating, *Science*, 348,  
327–331, <https://doi.org/10.1126/science.aaa0940>, 2015.
- Pattyn, F. and Morlighem, M.: The uncertain future of the Antarctic Ice Sheet, *Science*, 367, 1331-1335,  
695 <https://doi.org/10.1126/science.aaz5487>, 2020.
- Pfeffer, W. T., Arendt, A. A., Bliss, A., Bolch, T., Cogley, J. G., Gardner, A. S., Hagen, J.-O., Hock, R., Kaser,  
G., Kienholz, C., Miles, E. S., Moholdt, G., Mölg, N., Paul, F., Radić, V., Rastner, P., Raup, B. H., Rich, J., and  
Sharp, M. J.: The Randolph Glacier Inventory: a globally complete inventory of glaciers, *Journal of Glaciology*,  
700 60, 537-552, <https://doi.org/10.3189/2014JoG13J176>, 2014.

- Pritchard, H. D., Arthern, R. J., Vaughan, D. G., and Edwards, L. A.: Extensive dynamic thinning on the margins of the Greenland and Antarctic ice sheets, *Nature*, 461, 971-975, <https://doi.org/10.1038/nature08471>, 2009.
- 705 Rignot, E., Casassa, G., Gogineni, P., Krabill, W., Rivera, A., and Thomas, R.: Accelerated ice discharge from the Antarctic Peninsula following the collapse of Larsen B ice shelf, *Geophysical Research Letters*, 31, <https://doi.org/10.1029/2004GL020697>, 2004.
- Rignot, E. and Kanagaratnam, P.: Changes in the Velocity Structure of the Greenland Ice Sheet, *Science*, 311, 986–990, <https://doi.org/10.1126/science.1121381>, 2006.
- 710 Rignot, E., Mouginot, J., and Scheuchl, B.: Antarctic grounding line mapping from differential satellite radar interferometry, *Geophysical Research Letters*, 38, <https://doi.org/10.1029/2011GL047109>, 2011a.
- Rignot, E., Velicogna, I., van den Broeke, M. R., Monaghan, A., and Lenaerts, J. T. M.: Acceleration of the contribution of the Greenland and Antarctic ice sheets to sea level rise, *Geophysical Research Letters*, 38, <https://doi.org/10.1029/2011GL046583>, 2011.
- 715 Rignot, E., Mouginot, J., Scheuchl, B., van den Broeke, M., van Wessem, M. J., and Morlighem, M.: Four decades of Antarctic Ice Sheet mass balance from 1979-2017, *Proceedings Of The National Academy Of Sciences Of The United States Of America*, 116, 1095-1103, <https://doi.org/10.1073/pnas.1812883116>, 2019.
- 720 Ritz, C., Edwards, T. L., Durand, G., Payne, A. J., Peyaud, V., and Hindmarsh, R. C. A.: Potential sea-level rise from Antarctic ice-sheet instability constrained by observations, 528, 115–118, <https://doi.org/10.1038/nature16147>, 2015.
- 725 Riva, R. E. M., Gunter, B. C., Urban, T. J., Vermeersen, B. L. A., Lindenberg, R. C., Helsen, M. M., Bamber, J. L., van de Wal, R. S. W., van den Broeke, M. R., and Schutz, B. E.: Glacial Isostatic Adjustment over Antarctica from combined ICESat and GRACE satellite data, *Earth and Planetary Science Letters*, 288, <https://doi.org/10.1016/j.epsl.2009.10.013>, 516-523, 2009.
- 730 Sandberg Sørensen, L., Simonsen, S. B., Forsberg, R., Khvorostovsky, K., Meister, R., and Engdahl, M. E.: 25 years of elevation changes of the Greenland Ice Sheet from ERS, Envisat, and CryoSat-2 radar altimetry, *Earth and Planetary Science Letters*, 495, 234-241, <https://doi.org/10.1016/j.epsl.2018.05.015>, 2018.
- 735 Sasgen, I., Wouters, B., Gardner, A. S., King, M. D., Tedesco, M., Landerer, F. W., Dahle, C., Save, H., and Fettweis, X.: Return to rapid ice loss in Greenland and record loss in 2019 detected by the GRACE-FO satellites, *Commun Earth Environ*, 1, 1–8, <https://doi.org/10.1038/s43247-020-0010-1>, 2020.
- Selley, H. L., Hogg, A. E., Cornford, S., Dutrieux, P., Shepherd, A., Wuite, J., Floricioiu, D., Kusk, A., Nagler, T., Gilbert, L., Slater, T., and Kim, T.-W.: Widespread increase in dynamic imbalance in the Getz region of Antarctica from 1994 to 2018, 12, 1133, <https://doi.org/10.1038/s41467-021-21321-1>, 2021.
- 740

- Shepherd, A., Ivins, E. R., A. G., Barletta, V. R., Bentley, M. J., Bettadpur, S., Briggs, K. H., Bromwich, D. H., Forsberg, R., Galin, N., Horwath, M., Jacobs, S., Joughin, I., King, M. A., Jan, T. M. L., Li, J., Stefan, R. M. L., Luckman, A., Luthcke, S. B., McMillan, M., Meister, R., Milne, G., Mouginot, J., Muir, A., Nicolas, J. P., Paden, J., Payne, A. J., Pritchard, H., Rignot, E., Rott, H., Sørensen, L. S., Scambos, T. A., Scheuchl, B., Ernst, J. O. S., Smith, B., Sundal, A. V., Jan, H. v. A., Willem, J. v. d. B., Michiel, R. v. d. B., Vaughan, D. G., Velicogna, I., Wahr, J., Whitehouse, P. L., Wingham, D. J., Yi, D., Young, D., and Zwally, H. J.: A Reconciled Estimate of Ice-Sheet Mass Balance, *Science*, 338, 1183-1189, <https://doi.org/10.1126/science.1228102>, 2012.
- 745
- Shepherd, A. and Nowicki, S.: Improvements in ice-sheet sea-level projections, *Nature Climate Change*, 7, 672–674, <https://doi.org/10.1038/nclimate3400>, 2017.
- 750
- Shepherd, A., Gilbert, L., Muir, A. S., Konrad, H., McMillan, M., Slater, T., Briggs, K. H., Sundal, A. V., Hogg, A. E., and Engdahl, M. E.: Trends in Antarctic Ice Sheet Elevation and Mass, *Geophysical Research Letters*, 46, 8174–8183, <https://doi.org/10.1029/2019GL082182>, 2019.
- 755
- Slater, T., Hogg, A. E., and Mottram, R.: Ice-sheet losses track high-end sea-level rise projections, *Nature Climate Change*, 10, 879–881, <https://doi.org/10.1038/s41558-020-0893-y>, 2020.
- 760
- Slater, T., Shepherd, A., McMillan, M., Leeson, A., Gilbert, L., Muir, A., Munneke, P. K., Noël, B., Fettweis, X., van den Broeke, M., and Briggs, K.: Increased variability in Greenland Ice Sheet runoff from satellite observations, *Nat Commun*, 12, 6069, <https://doi.org/10.1038/s41467-021-26229-4>, 2021.
- Small, D., Bentley, M.J., Jones, R.S., Pittard, M.L., and Whitehouse, P.L.: Antarctic ice sheet palaeo-thinning rates from vertical transects of cosmogenic exposure ages, *Quat. Sci. Rev*, 206, 65–80, <https://doi.org/10.1016/j.quascirev.2018.12.024>, 2019.
- 765
- Smith, B., Fricker, H. A., Gardner, A. S., Medley, B., Nilsson, J., Paolo, F. S., Holschuh, N., Adusumilli, S., Brunt, K., Csatho, B., Harbeck, K., Markus, T., Neumann, T., Siegfried, M. R., and Zwally, H. J.: Pervasive ice sheet mass loss reflects competing ocean and atmosphere processes, *Science*, 368, 1239-1242, <https://doi.org/10.1126/science.aaz5845>, 2020.
- 770
- Sørensen, L. S., Simonsen, S. B., Nielsen, K., Lucas-Picher, P., Spada, G., Adalgeirsdottir, G., Forsberg, R., and Hvidberg, C. S.: Mass balance of the Greenland ice sheet (2003–2008) from ICESat data – the impact of interpolation, sampling and firn density, *The Cryosphere*, 5, 173–186, <https://doi.org/10.5194/tc-5-173-2011>, 2011.
- 775
- Stevens, C. M., Verjans, V., Lundin, J. M. D., Kahle, E. C., Horlings, A. N., Horlings, B. I., and Waddington, E. D.: The Community Firn Model (CFM) v1.0, *Geoscientific Model Development*, 13(9), 4355-4377, 2020.
- Straneo, F. and Heimbach, P.: North Atlantic warming and the retreat of Greenland’s outlet glaciers, *Nature*, 504,

- 780 36–43, <https://doi.org/10.1038/nature12854>, 2013.
- Sutterley, T. C., Velicogna, I., Csatho, B., van den Broeke, M., Rezvan-Behbahani, S., and Babonis, G.: Evaluating Greenland glacial isostatic adjustment corrections using GRACE, altimetry and surface mass balance data, *Environmental Research Letters*, 9, 014004, <https://doi.org/10.1088/1748-9326/9/1/014004>, 2014a.
- 785 Sutterley, T. C., Velicogna, I., Rignot, E., Mouginot, J., Flament, T., Van Den Broeke, M. R., info:eu, r. d. n., Van Wessem, J. M., Reijmer, C. H., and info:eu, r. d. n.: Mass loss of the Amundsen Sea Embayment of West Antarctica from four independent techniques, *Geophysical Research Letters*, 41, 8421-8428, <https://doi.org/10.1002/2014GL061940>, 2014b.
- 790 Tapley, B. D., Watkins, M. M., Flechtner, F., Reigber, C., Bettadpur, S., Rodell, M., Sasgen, I., Famiglietti, J. S., Landerer, F. W., Chambers, D. P., Reager, J. T., Gardner, A. S., Save, H., Ivins, E. R., Swenson, S. C., Boening, C., Dahle, C., Wiese, D. N., Dobslaw, H., Tamisiea, M. E., and Velicogna, I.: Contributions of GRACE to understanding climate change, *Nature Climate Change*, 5, 358-369, <https://doi.org/10.1038/s41558-019-0456-2>, 2019.
- 795 Tedesco, M. and Fettweis, X.: Unprecedented atmospheric conditions (1948–2019) drive the 2019 exceptional melting season over the Greenland ice sheet, *The Cryosphere*, 14, 1209–1223, <https://doi.org/10.5194/tc-14-1209-2020>, 2020.
- Trusel, L. D., Das, S. B., Osman, M. B., Evans, M. J., Smith, B. E., Fettweis, X., McConnell, J. R., Noël, B. P. Y., and Broeke, M. R. van den: Nonlinear rise in Greenland runoff in response to post-industrial Arctic warming, *Nature*, 564, 104–108, <https://doi.org/10.1038/s41586-018-0752-4>, 2018.
- 800 Velicogna, I., Mohajerani, Y., Geruo, A., Landerer, F., Mouginot, J., Noel, B., Rignot, E., Sutterley, T., van den Broeke, M., van Wessem, J. M., and Wiese, D.: Continuity of ice sheet mass loss in Greenland and Antarctica from the GRACE and GRACE Follow-Onmissions, *Geophysical Research Letters*, 47, e2020GL087291, <https://doi.org/10.1029/2020gl087291>, 2020.
- 805 Velicogna I and Wahr J: Measurements of time-variable gravity show mass loss in Antarctica. *Science*, 2006, 311, 1754-1756, <https://doi.org/10.1126/science.1123785>, 2006.
- 810 Vishwakarma, B. D., Ziegler, Y., Bamber, J. L., and Royston, S.: Separating GIA signal from surface mass change using GPS and GRACE data, *Geophysical Journal International*, 232, 537-547, <https://doi.org/10.1093/gji/ggac336>, 2022.
- 815 Vitousek, S., Barnard, P. L., Fletcher, C. H., Frazer, N., Erikson, L., and Storlazzi, C. D.: Doubling of coastal flooding frequency within decades due to sea-level rise, *Sci Rep*, 7, 1–9, <https://doi.org/10.1038/s41598-017-01362-7>, 2017.

820 Wang, L., Davis, J. L., and Howat, I. M.: Complex Patterns of Antarctic Ice Sheet Mass Change Resolved by  
 Time-Dependent Rate Modeling of GRACE and GRACE Follow-On Observations, *Geophysical Research  
 Letters*, 48, e2020GL090961, <https://doi.org/10.1029/2020GL090961>, 2021.

825 Wcrp Global Sea Level Budget Group: Global sea-level budget 1993–present, *Earth Syst. Sci. Data*, 10, 1551-  
 1590, <https://doi.org/10.5194/essd-10-1551-2018>, 2018.

Whitehouse, P. L.: Glacial isostatic adjustment modelling: historical perspectives, recent advances, and future  
 directions, *Earth Surf. Dynam.*, 6, 401-429, <https://doi.org/10.5194/esurf-6-401-2018>, 2018.

830 Wingham, D. J., Ridout, A. J., Scharroo, R., Arthern, R. J., and Shum, C. K.: Antarctic Elevation Change from  
 1992 to 1996, *Science*, 282, 456-458, <https://doi.org/10.1126/science.282.5388.456>, 1998.

Zwally, H. J., Giovinetto, M. B., Beckley, M. A. and Saba, J. L: Antarctic and Greenland Drainage Systems,  
 GSFC Cryospheric Sciences Laboratory, [http://icesat4.gsfc.nasa.gov/cryo\\_data/ant\\_grn\\_drainage\\_systems.php](http://icesat4.gsfc.nasa.gov/cryo_data/ant_grn_drainage_systems.php),  
 2012.

835

840

**Appendix A**

845

<b>Table A1. References of the datasets, methods, GIA and SMB models employed by participants of the input-output, altimetry and gravimetry experiment groups.</b>		
<b>IOM</b>	Andersen	Andersen, M. L. <i>et al.</i> Basin-scale partitioning of Greenland ice sheet mass balance components (2007–2011). <i>Earth and Planetary Science Letters</i> <b>409</b> , 89–95 (2015).
	Colgan	Colgan, W. <i>et al.</i> Greenland ice sheet mass balance assessed by PROMICE (1995–2015). <i>Geological Survey of Denmark and Greenland Bulletin</i> <b>43</b> (2019).
	Mouginot	Mouginot, J. <i>et al.</i> Forty-six years of Greenland Ice Sheet mass balance from 1972 to 2018. <i>PNAS</i> <b>116</b> , 9239–9244 (2019).

	Rignot	Rignot E. <i>et al.</i> Four decades of Antarctic Ice Sheet mass balance from 1979-2017. <i>PNAS</i> <b>116</b> (4), 1095-1103 (2019).
ALT	Gourmelen	Gourmelen, N. <i>et al.</i> CryoSat-2 swath interferometric altimetry for mapping ice elevation and elevation change. <i>Advances in Space Research</i> <b>62</b> , 1226–1242 (2018).
	Gunter	Gunter, B. C. <i>et al.</i> Empirical estimation of present-day Antarctic glacial isostatic adjustment and ice mass change. <i>The Cryosphere</i> <b>8</b> , 743–760 (2014).
	Helm	Helm, V., Humbert, A. & Miller, H. Elevation and elevation change of Greenland and Antarctica derived from CryoSat-2. <i>The Cryosphere</i> <b>8</b> , 1539–1559 (2014).
	Khan	Khan, S. A. <i>et al.</i> Sustained mass loss of the northeast Greenland ice sheet triggered by regional warming. <i>Nature Climate Change</i> <b>4</b> , 292–299 (2014).
	McMillan	McMillan, M. <i>et al.</i> A high-resolution record of Greenland mass balance. <i>Geophysical Research Letters</i> <b>43</b> , 7002–7010 (2016).
	Nilsson Gardner	Nilsson, J., Gardner, A., Sandberg Sørensen, L. & Forsberg, R. Improved retrieval of land ice topography from CryoSat-2 data and its impact for volume-change estimation of the Greenland Ice Sheet. <i>The Cryosphere</i> <b>10</b> , 2953–2969 (2016).
	Pie	Felikson, D. <i>et al.</i> Comparison of Elevation Change Detection Methods From ICESat Altimetry Over the Greenland Ice Sheet. <i>IEEE Transactions on Geoscience and Remote Sensing</i> <b>55</b> , 5494–5505 (2017).
	Sandberg Sørensen	Sørensen, L. S. <i>et al.</i> Mass balance of the Greenland ice sheet (2003–2008) from ICESat data – the impact of interpolation, sampling and firn density. <i>The Cryosphere</i> <b>5</b> , 173–186 (2011).
	Schroder	Schröder, L. <i>et al.</i> Four decades of Antarctic surface elevation changes from multi-mission satellite altimetry." <i>The Cryosphere</i> <b>13</b> (2), 427-449, (2019).
	Shepherd	Shepherd, A. <i>et al.</i> Trends in Antarctic Ice Sheet Elevation and Mass. <i>Geophysical Research Letters</i> <b>46</b> (14), 8174-8183 (2019).
Zwally	Zwally, H. J. <i>et al.</i> Mass gains of the Antarctic ice sheet exceed losses. <i>J. Glaciol.</i> <b>61</b> , 1019-1036 (2015).	
GMB	Blazquez	Blazquez, A. <i>et al.</i> Exploring the uncertainty in GRACE estimates of the mass redistributions at the Earth surface: implications for the global water and sea level budgets. <i>Geophys J Int</i> <b>215</b> , 415–430 (2018).
	Bonin	Bonin, J. & Chambers, D. Uncertainty estimates of a GRACE inversion modelling technique over Greenland using a simulation. <i>Geophys J Int</i> <b>194</b> , 212–229 (2013).

Forsberg	Forsberg, R., Sørensen, L. & Simonsen, S. Greenland and Antarctica Ice Sheet Mass Changes and Effects on Global Sea Level. <i>Surv Geophys</i> <b>38</b> , 89–104 (2017).
Gardner Nilsson	Gardner, A. S. <i>et al.</i> Increased West Antarctic and unchanged East Antarctic ice discharge over the last 7 years. <i>The Cryosphere</i> <b>12</b> (2), 521-547 (2018).
Groh	Groh, A., & Horwath, M. Antarctic Ice Mass Change Products from GRACE/GRACE-FO Using Tailored Sensitivity Kernels. <i>Remote Sensing</i> , <b>13</b> , 1736, <a href="https://doi.org/10.3390/rs13091736">https://doi.org/10.3390/rs13091736</a> (2021).
Harig	Harig, C. & Simons, F. J. Mapping Greenland’s mass loss in space and time. <i>PNAS</i> <b>109</b> , 19934–19937 (2012).
Horvath	Horvath, A. G. Retrieving Geophysical Signals from Current and Future Satellite Missions. PhD thesis, Tech. Univ. Munich (2017).
Luthcke	Luthcke, S. B. <i>et al.</i> Antarctica, Greenland and Gulf of Alaska land-ice evolution from an iterated GRACE global mascon solution. <i>Journal of Glaciology</i> <b>59</b> , 613–631 (2013).
Moore	Andrews, S. B., Moore, P. & King, M. A. Mass change from GRACE: a simulated comparison of Level-1B analysis techniques. <i>Geophys J Int</i> <b>200</b> , 503–518 (2015).
Save	Save, H., Bettadpur, S. & Tapley, B. D. High-resolution CSR GRACE RL05 mascons. <i>Journal of Geophysical Research: Solid Earth</i> <b>121</b> , 7547–7569 (2016).
Schrama	Schrama, E. J. O., Wouters, B. & Rietbroek, R. A mascon approach to assess ice sheet and glacier mass balances and their uncertainties from GRACE data. <i>Journal of Geophysical Research: Solid Earth</i> <b>119</b> , 6048–6066 (2014).
Seo	Seo, K.-W. <i>et al.</i> Surface mass balance contributions to acceleration of Antarctic ice mass loss during 2003–2013. <i>Journal of Geophysical Research: Solid Earth</i> <b>120</b> , 3617–3627 (2015).
Velicogna	Velicogna, I., Sutterley, T. C. & Broeke, M. R. van den. Regional acceleration in ice mass loss from Greenland and Antarctica using GRACE time-variable gravity data. <i>Geophysical Research Letters</i> <b>41</b> , 8130–8137 (2014).
Vishwakarma	Vishwakarma, B. D., Horwath, M., Devaraju, B., Groh, A. & Sneeuw, N. A Data-Driven Approach for Repairing the Hydrological Catchment Signal Damage Due to Filtering of GRACE Products. <i>Water Resources Research</i> <b>53</b> , 9824–9844 (2017).
Wiese	Wiese, D. N., Landerer, F. W. & Watkins, M. M. Quantifying and reducing leakage errors in the JPL RL05M GRACE mascon solution. <i>Water Resources Research</i> <b>52</b> , 7490–7502 (2016).
Wouters	Wouters, B., Bamber, J. L., van den Broeke, M. R., Lenaerts, J. T. M. & Sasgen, I. Limits in



		detecting acceleration of ice sheet mass loss due to climate variability. <i>Nature Geoscience</i> <b>6</b> , 613–616 (2013).
GIA	A13	A, Geruo, John Wahr, Shijie Zhong, Computations of the viscoelastic response of a 3-D compressible Earth to surface loading: an application to Glacial Isostatic Adjustment in Antarctica and Canada, <i>Geophysical Journal International</i> , Volume 192, Issue 2, February 2013, Pages 557–572, <a href="https://doi.org/10.1093/gji/ggs030">https://doi.org/10.1093/gji/ggs030</a>
	W12a	Whitehouse, Pippa L., Michael J. Bentley, Glenn A. Milne, Matt A. King, Ian D. Thomas, A new glacial isostatic adjustment model for Antarctica: calibrated and tested using observations of relative sea-level change and present-day uplift rates, <i>Geophysical Journal International</i> , Volume 190, Issue 3, September 2012, Pages 1464–1482, <a href="https://doi.org/10.1111/j.1365-246X.2012.05557.x">https://doi.org/10.1111/j.1365-246X.2012.05557.x</a>
	ICE-5G	Peltier, W. R. (2004). "Global Glacial Isostasy And The Surface Of The Ice-Age Earth: The ICE-5G (VM2) Model and GRACE." <i>Annual Review of Earth and Planetary Sciences</i> <b>32</b> (1): 111-149.
	ICE-6G	Peltier, W. R., Argus, D. F., & Drummond, R. (2015). Space geodesy constrains ice age terminal deglaciation: The global ICE-6G_C (VM5a) model. <i>Journal of Geophysical Research: Solid Earth</i> , <i>120</i> (1), 450-487.
	IJ05	Ivins, E., & James, T. (2005). Antarctic glacial isostatic adjustment: A new assessment. <i>Antarctic Science</i> , <i>17</i> (4), 541-553. doi:10.1017/S095410200500296)
	IJ05_R2	Ivins, E. R., T. S. James, J. Wahr, E. J.O. Schrama, F.W. Landerer & K. M. Simon, Antarctic contribution to sea-level rise observed by GRACE with improved GIA correction, <i>J. Geophys. Res., B - Solid Earth</i> , <i>118</i> , 3126-3141, doi:10.1002/jgrb.50208 (2013).
	Paulson07	Paulson, A., Zhong, S. and Wahr, J. (2007), Inference of mantle viscosity from GRACE and relative sea level data. <i>Geophysical Journal International</i> , <i>171</i> : 497-508. <a href="https://doi.org/10.1111/j.1365-246X.2007.03556.x">https://doi.org/10.1111/j.1365-246X.2007.03556.x</a>
	Simpson09	Simpson, M. J. R. and Milne, G. A. and Huybrechts, P. and Long, A. J. (2009) 'Calibrating a glaciological model of the Greenland ice sheet from the last glacial maximum to present-day using field observations of relative sea level and ice extent.', <i>Quaternary science reviews.</i> , <i>28</i> (17-18). pp. 1631-1657.
	Khan_2016	Khan, S. A., I. Sasgen, M. Bevis, T. v. Dam, J. L. Bamber, J. Wahr, M. Willis, K. H. Kjær, B. Wouters, V. Helm, B. Csatho, K. Fleming, A. A. Björk, A. Aschwanden, P. Knudsen and P. K. Munneke (2016). "Geodetic measurements reveal similarities between post-Last Glacial Maximum and present-day mass loss from the Greenland ice sheet." <i>Science Advances</i> <b>2</b> (9): e1600931.

	Schrama14	Schrama, E. J. O., Wouters, B., and Rietbroek, R. (2014), A mascon approach to assess ice sheet and glacier mass balances and their uncertainties from GRACE data, <i>J. Geophys. Res. Solid Earth</i> , 119, 6048– 6066, doi: <a href="https://doi.org/10.1002/2013JB010923">10.1002/2013JB010923</a> .
<b>SMB</b>	RACMO 2.3	Van Wessem, J. M., Reijmer, C. H., Morlighem, M., Mouginot, J., Rignot, E., Medley, B., Joughin, I., Wouters, B., Depoorter, M. A., Bamber, J. L., Lenaerts, J. T. M., Van De Berg, W. J., Van Den Broeke, M. R. and Van Meijgaard, E. (2014) “Improved representation of East Antarctic surface mass balance in a regional atmospheric climate model,” <i>Journal of Glaciology</i> , Cambridge University Press, 60(222), pp. 761–770.
	MAR 3.5	Fettweis, X., B. Franco, M. Tedesco, J. H. van Angelen, J. T. M. Lenaerts, M. R. van den Broeke and H. Gallée (2013). "Estimating the Greenland ice sheet surface mass balance contribution to future sea level rise using the regional atmospheric climate model MAR." <i>The Cryosphere</i> 7(2): 469-489.

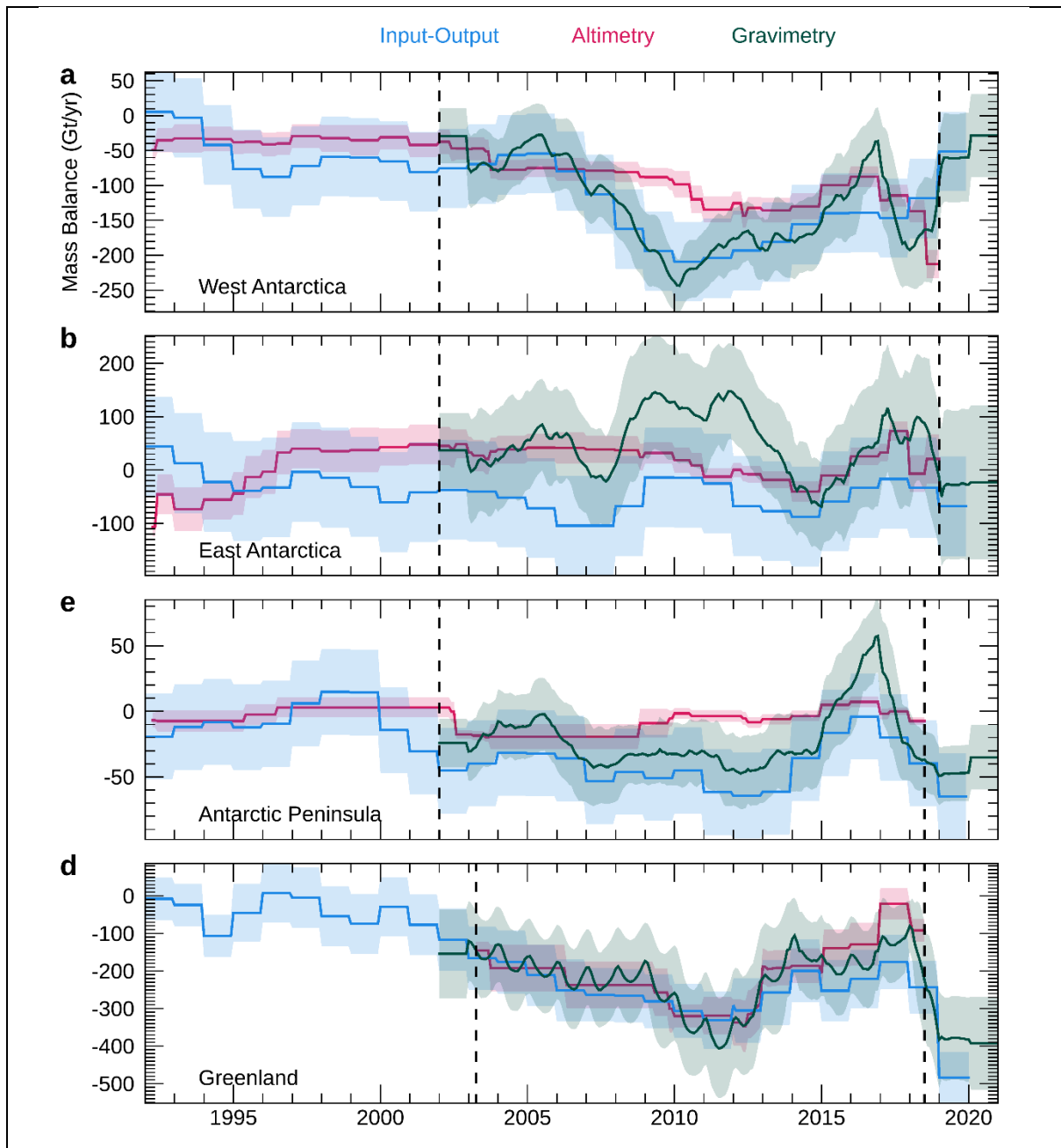


**Figure A1.** Mass balance time-series from the aggregated altimetry, gravimetry and input-output method over the a) WAIS, b) EAIS, c) APIS, and d) GrIS. The vertical dashed lines mark the overlap period of the three time-series. The aggregated time-series and corresponding uncertainties are calculated following the methods described in Section 3 (ii).

**Table A2.** Rates of mass change (in  $\text{Gt yr}^{-1}$ ) over the gravimetry record (2002 to 2020) from our reconciled estimate and from a modified version of our reconciled estimate in which the contribution of the peripheral glaciers has been removed from the gravimetry estimates following the method described in Section 3.

	Reconciled assessment	Modified reconciled assessment
<b>GrIS</b>	$-235.6 \pm 20.6$	$-226.0 \pm 20.6$
<b>APIS</b>	$-18.3 \pm 6.0$	$-15.7 \pm 5.8$
<b>EAIS</b>	$6.1 \pm 19.7$	$6.2 \pm 19.6$
<b>WAIS</b>	$-104.8 \pm 11.2$	$-103.6 \pm 10.8$
<b>AIS</b>	$-117.0 \pm 23.5$	$-113.1 \pm 23.2$